

Atomistic simulations with applications to Si and Ge systems

J. Hickman

NRC Postdoctoral fellow
MML

NIST: Gaithersburg MD

2018 Atomistic Simulations for Industrial Needs Workshop
August 01-03, Rockville, MD

NIST

National Institute of
Standards and Technology
U.S. Department of Commerce



Presentation Overview

- **Physically informed neural network (PINN) interatomic potentials (Mishin 2017)**
 - **Motivation and Introduction**
 - **Overview of potential model**
 - **Training set generation**
 - **Potential Development/training process**
 - **Si PINN results**
 - **AI PINN results**
 - **Future work (SiGe)**

Introduction

Motivation

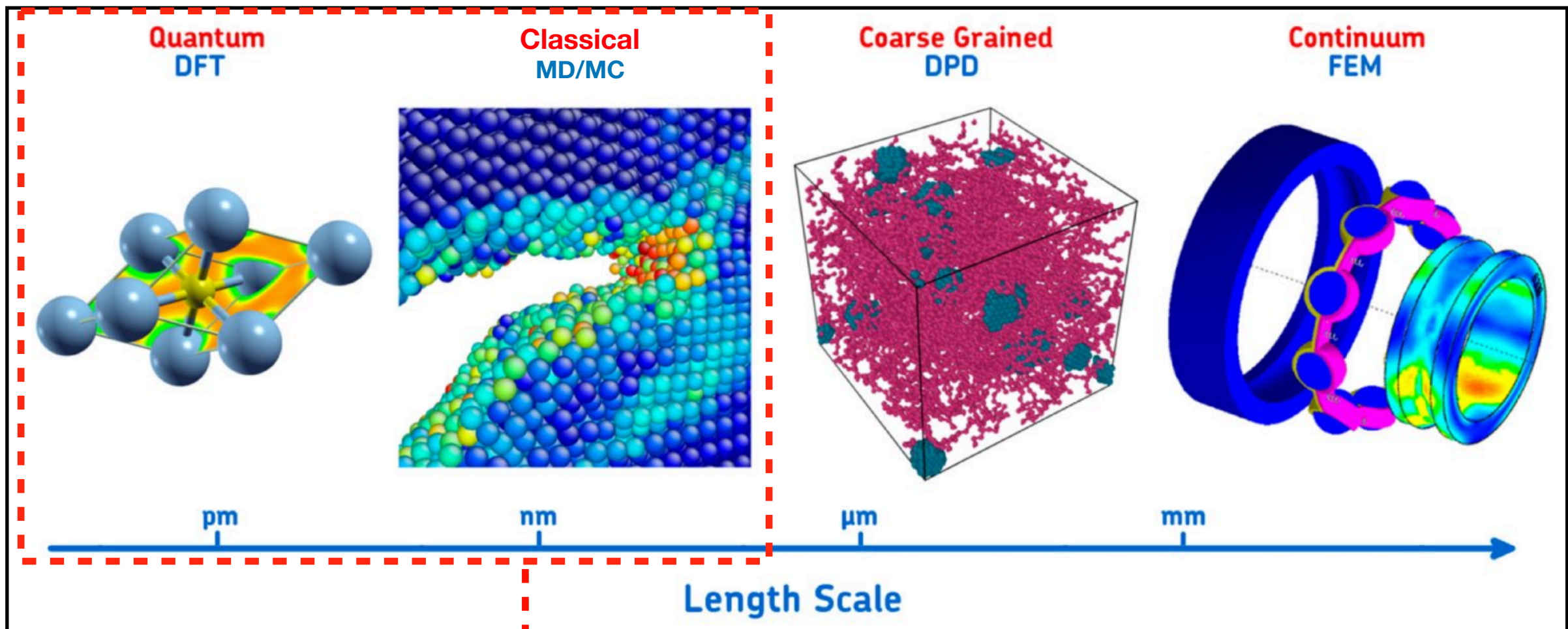


image source: <http://evolution.skf.com/us/bearing-research-going-to-the-atomic-scale>

Ab-initio/DFT

- Slow
- Size limited ($N \sim 10^2$)
- 0K or short timescales
- Very accurate

Compromises

Speed
Accuracy
Scalability
Transferability

Classical (MD/MC)

- Fast
- Larger systems ($N \sim 10^7$)
- Kinetic phenomena/long simulations
- ★ Accuracy depends on *approximation* of the potential energy surface (PES)

Better potential models

$$E = E(\mathbf{r}_1, \dots, \mathbf{r}_N)$$

Types of interatomic potentials

Traditional interatomic potential

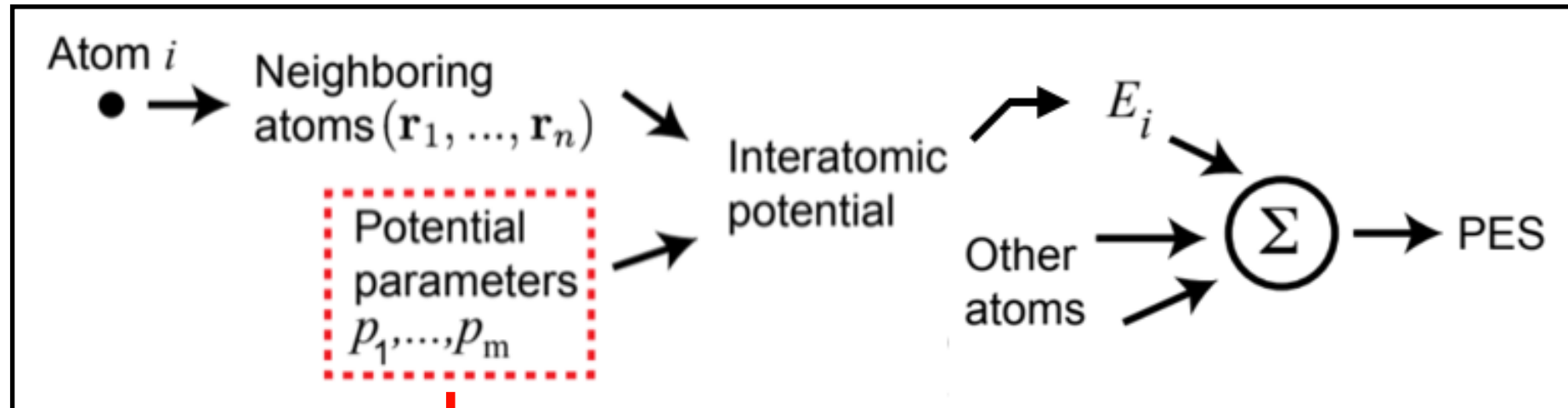


image source: Y. Mishin, 2017, ONR proposal

$$E = E(\mathbf{r}_1, \dots, \mathbf{r}_N)$$

-EAM, ADP, REAX, COMB, REBO, REAXFF ... etc

-PES approximated via physically derived analytic functions

~10-20 parameters

Fit or “train” the potential parameters using experimental and DFT data

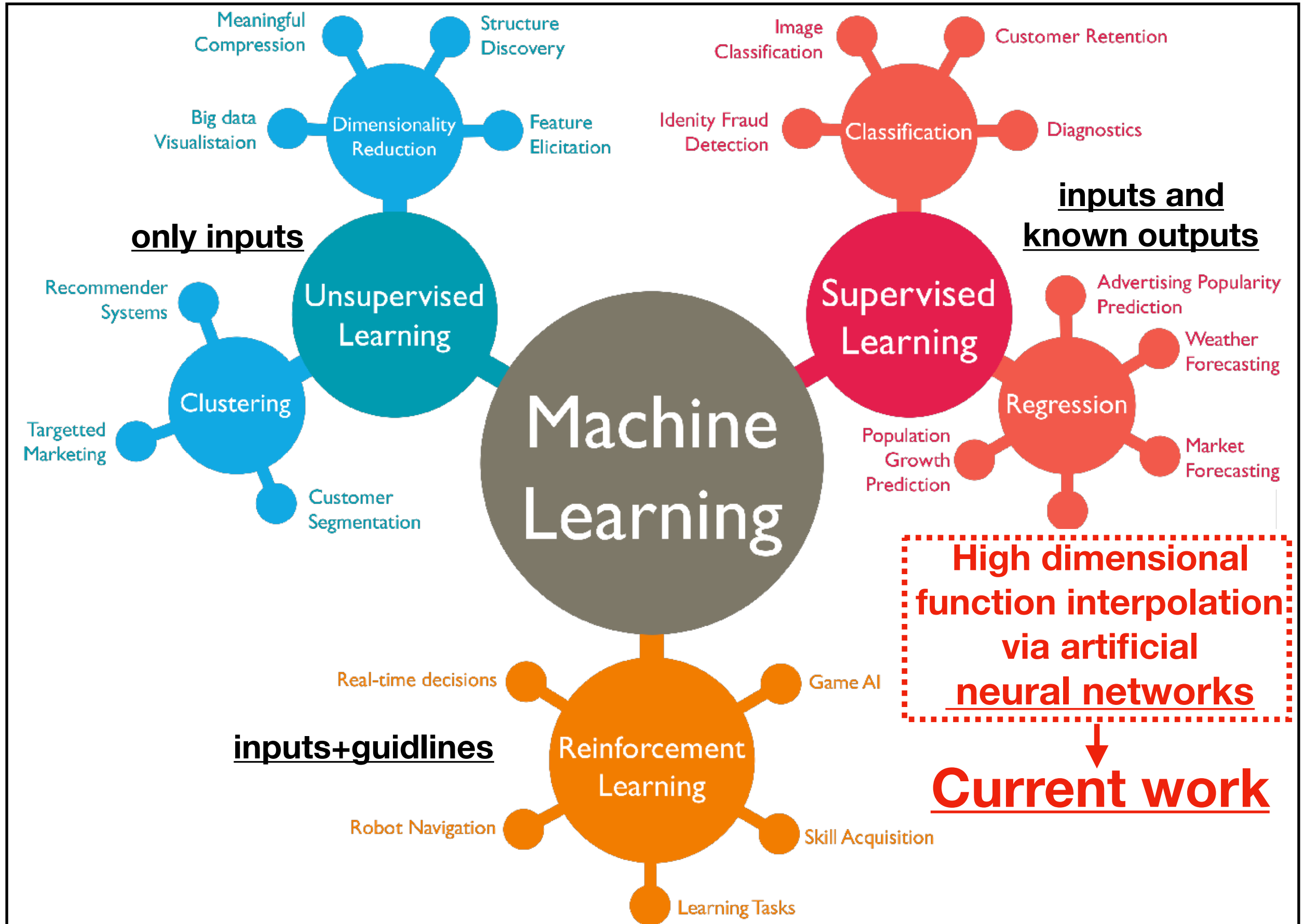
Machine learning potentials →

Approximate PES via DFT energy or force interpolation

- Gaussian process regression
- Interpolating moving least squares
- Kernel ridge regression
- Compressed sensing

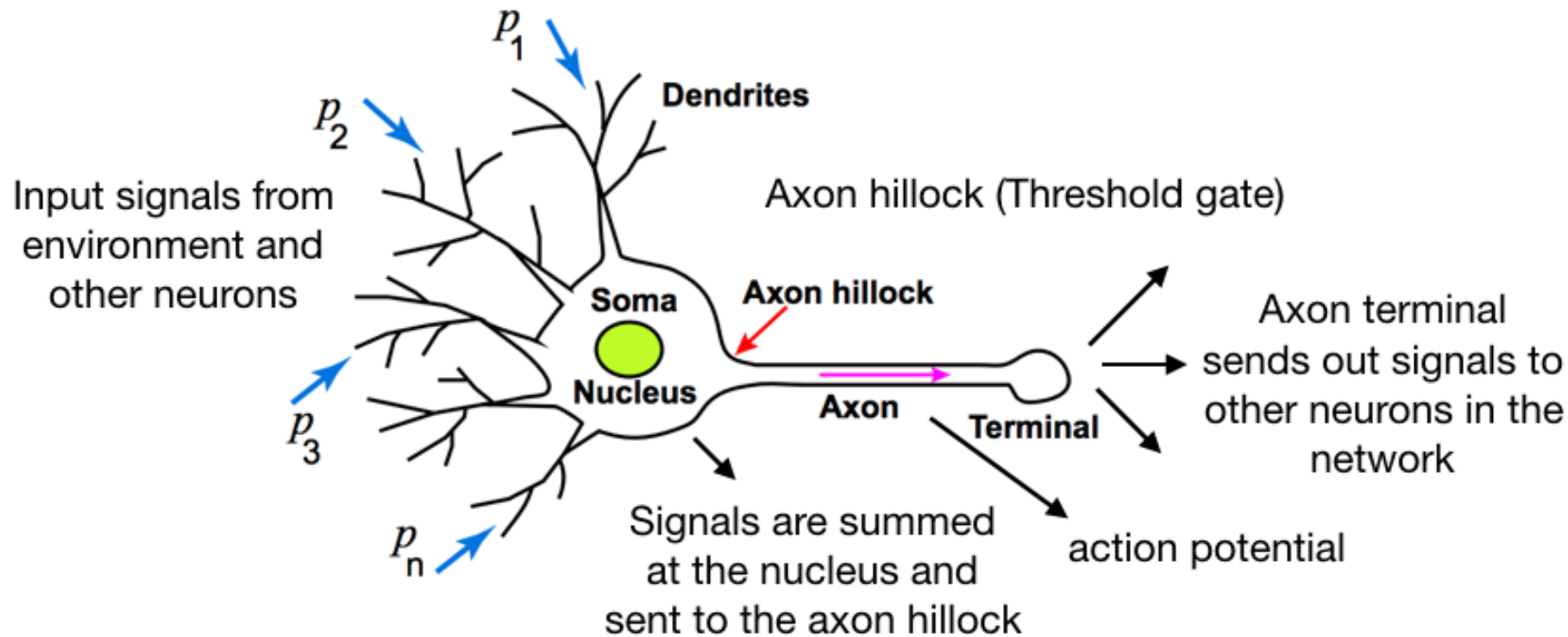
★ Artificial neural network (ANN) potentials

Types of machine learning applications

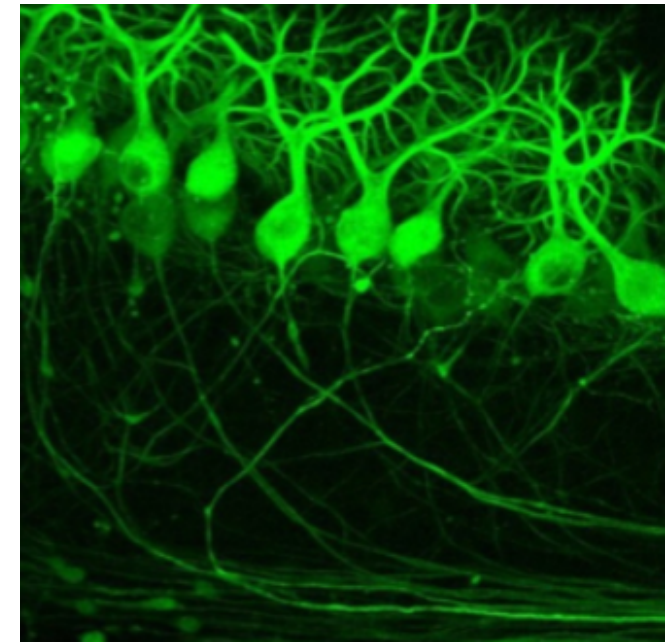


Neural networks-1

Biological neuron

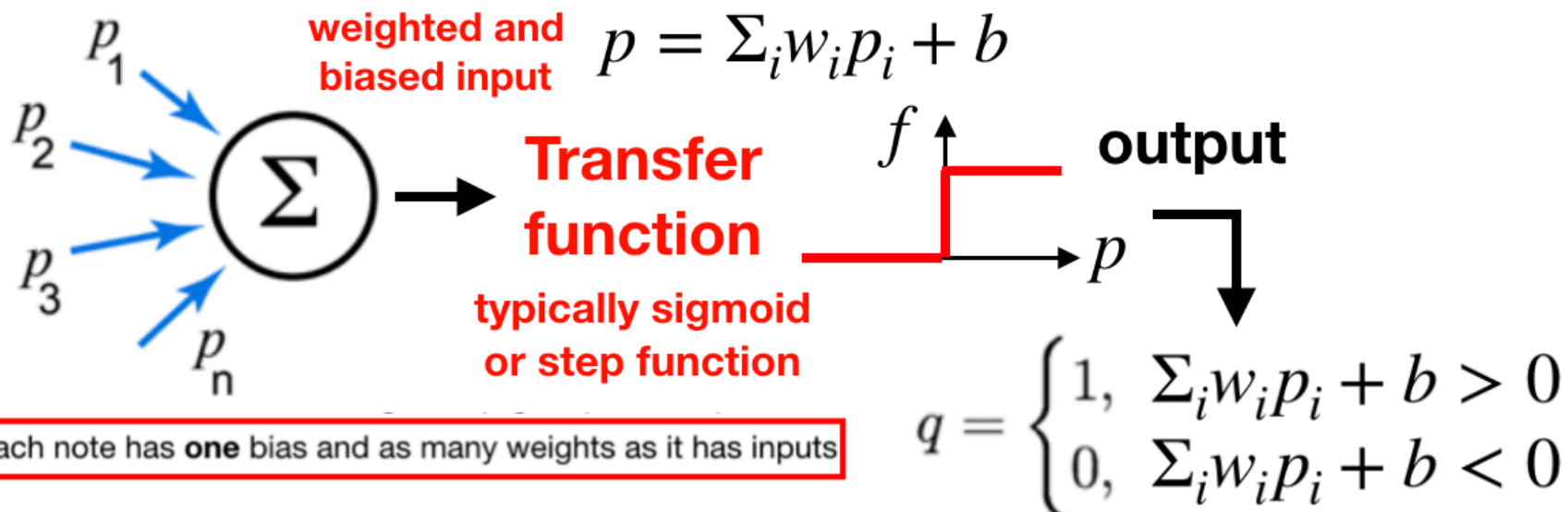


Biological neural network

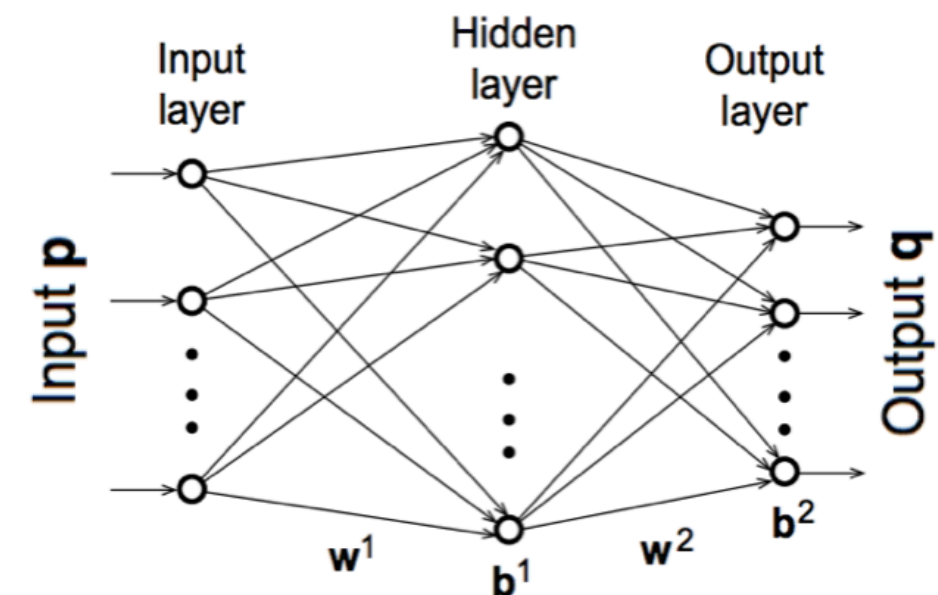


Artificial neuron

AKA: nodes or perceptrons

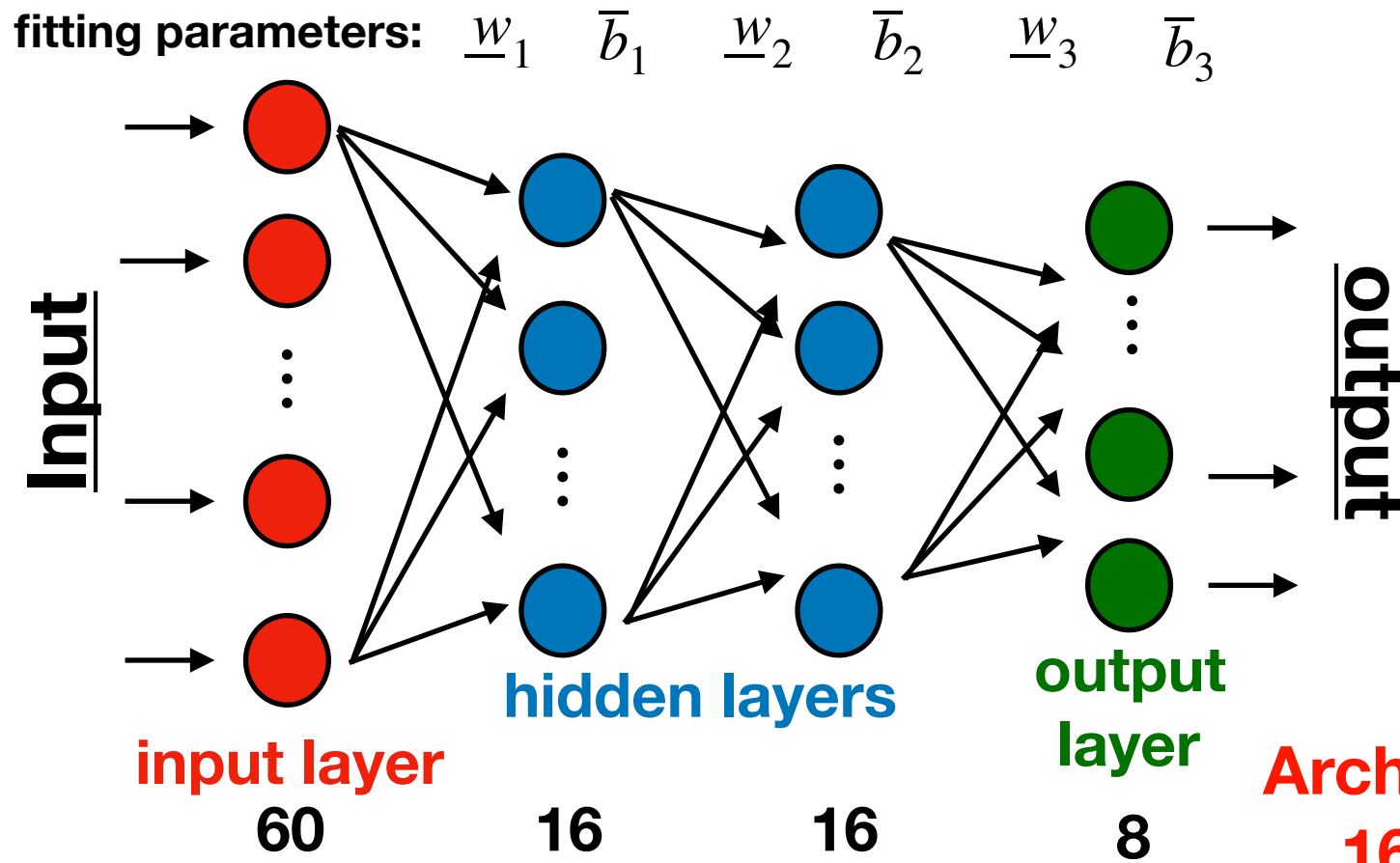


Artificial neural network



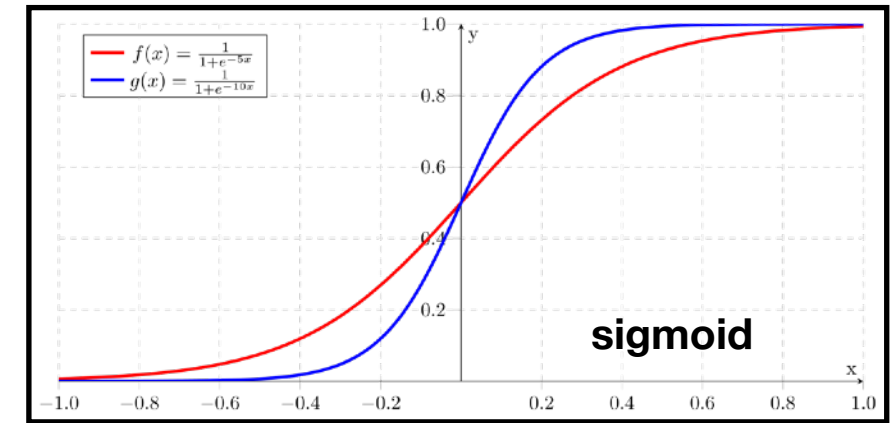
Neural networks-2

Architecture:



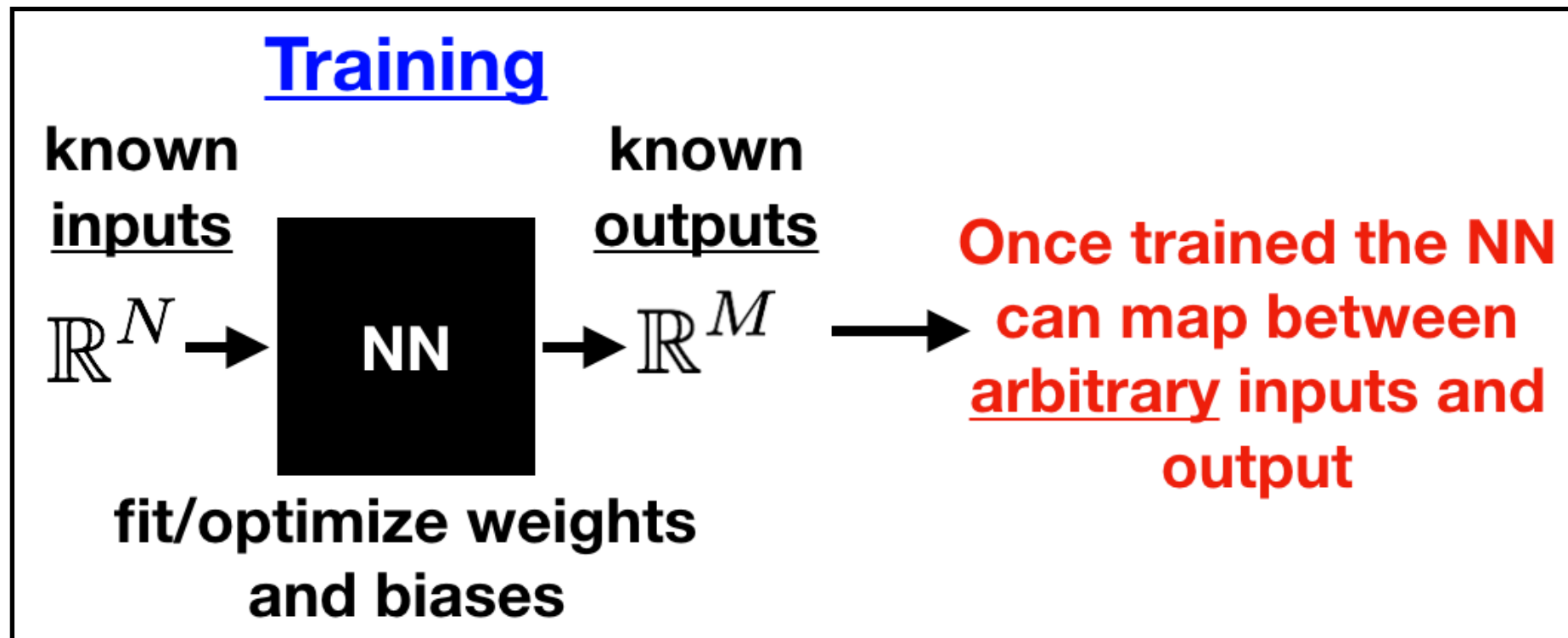
Network description/architecture
layers+transfer functions+weights and biases

Transfer function: $f(p) = \frac{1}{1 + e^{-p}}$



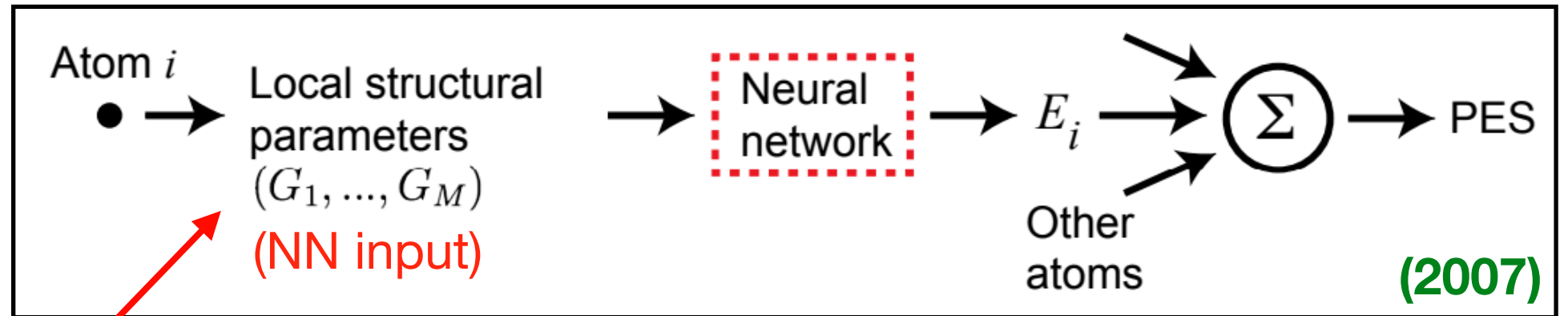
Architecture:
16x16x8

$N_{fit} = (60 \times 16 + 16) + (16 \times 16 + 16) + (16 \times 8 + 8) = \boxed{1384}$ **Number of NN fitting parameters**



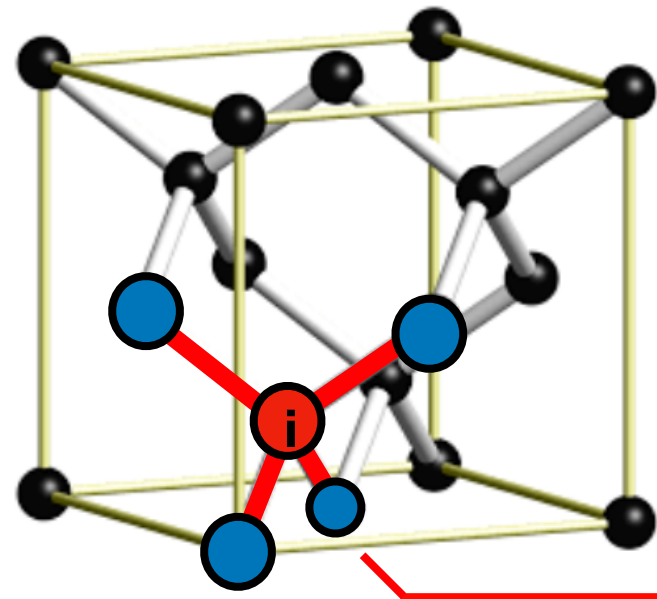
Artificial neural network potentials

“Mathematical” or “straight NN potential model:



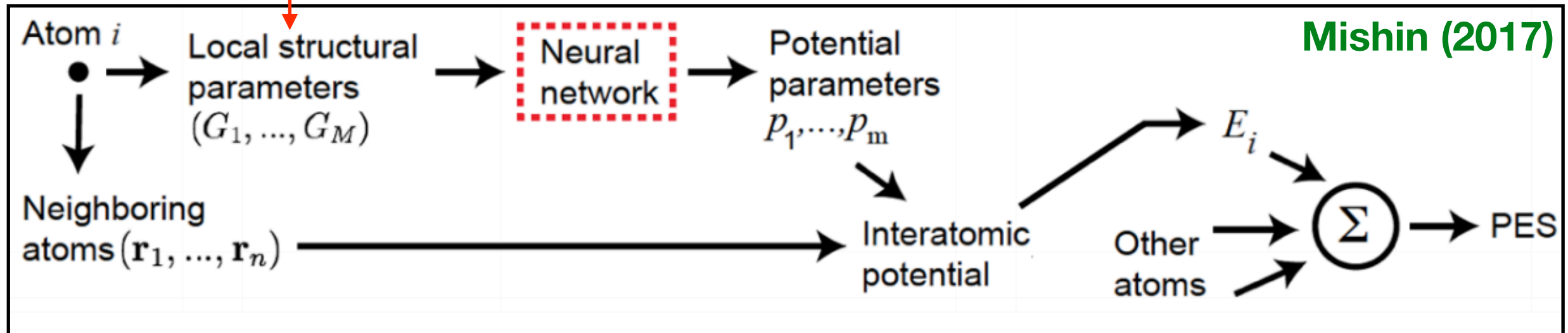
[33] J. Behler, M. Parrinello, Generalized neural-network representation of high-dimensional potential-energy surfaces, *Phys. Rev. Lett.* 98 (2007) 146401.

[34] A. Bholoa, S. D. Kenny, R. Smith, A new approach to potential fitting using neural networks, *Nucl. Instrum. Methods Phys. Res.* 255 (2007) 1–7.



Quantify local structural “fingerprint”

Physically informed neural network (PINN) potential model:



Mishin (2017)

Training process:

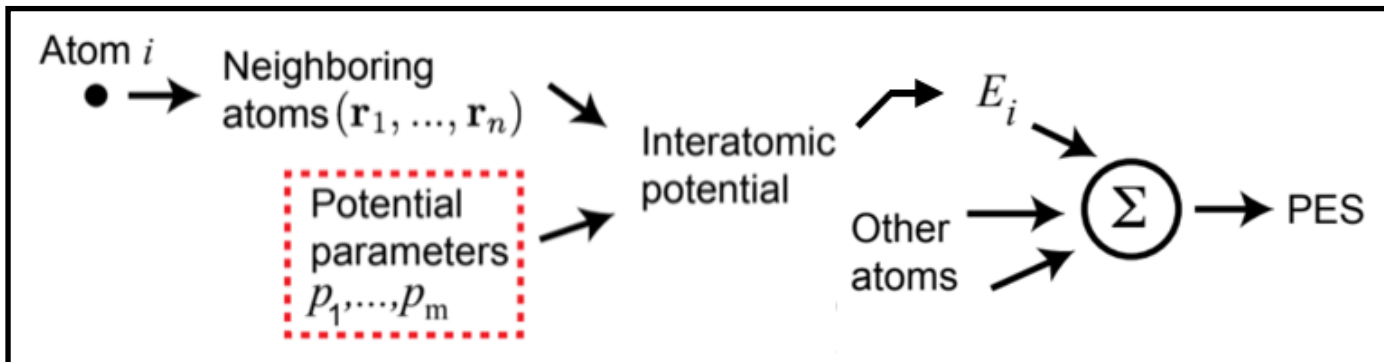
“Training set”
 Structures DFT energies Model error → RMSE = $\left(\frac{\sum_i (E_i - \tilde{E}_i)^2}{N} \right)^{\frac{1}{2}}$ Fitting
 Structures DFT energies Model energies

config-1	E_1	\tilde{E}_1
config-2	E_2	\tilde{E}_2
⋮	⋮	⋮
config-N	E_N	\tilde{E}_N

Find the NN weights and bias's which minimize the RMSE

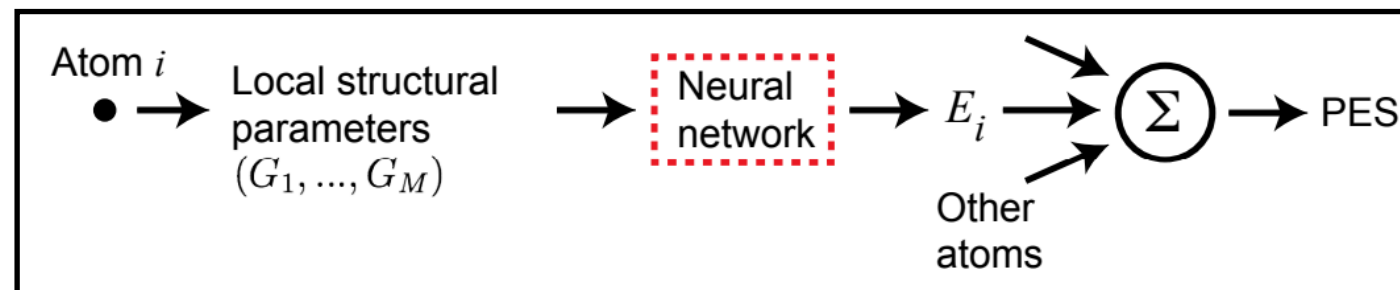
Potential model comparison

Traditional interatomic potential:

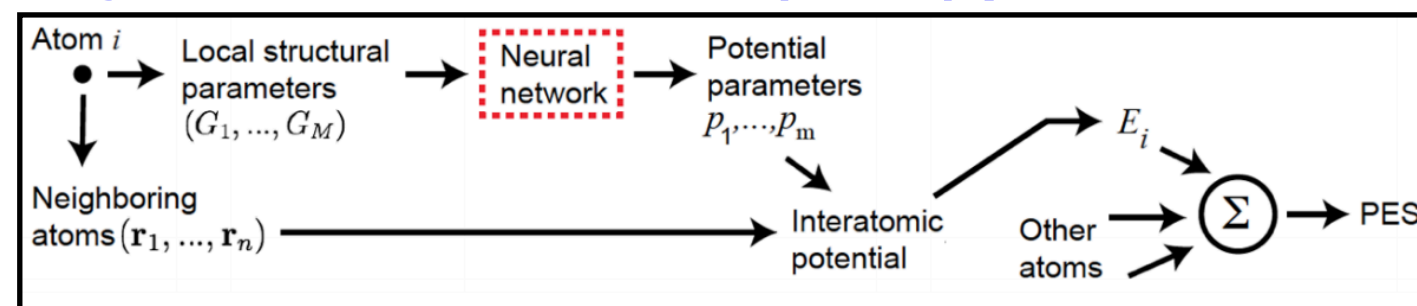


- extrapolation=predictions outside training region

“Mathematical” or “straight NN potential:



Physical neural network (PINN) potential:



Pros

- Very fast
- Decent extrapolation
- Potential models derived from physics
- Fast relative to DFT
- DFT level accuracy (~1-5 mEv) within training set
- Relatively straight forward/routine to train/fit
- Systematic improvement (add more data)
- Same as straight NN
- Decent extrapolation
- Potential models derived from physics

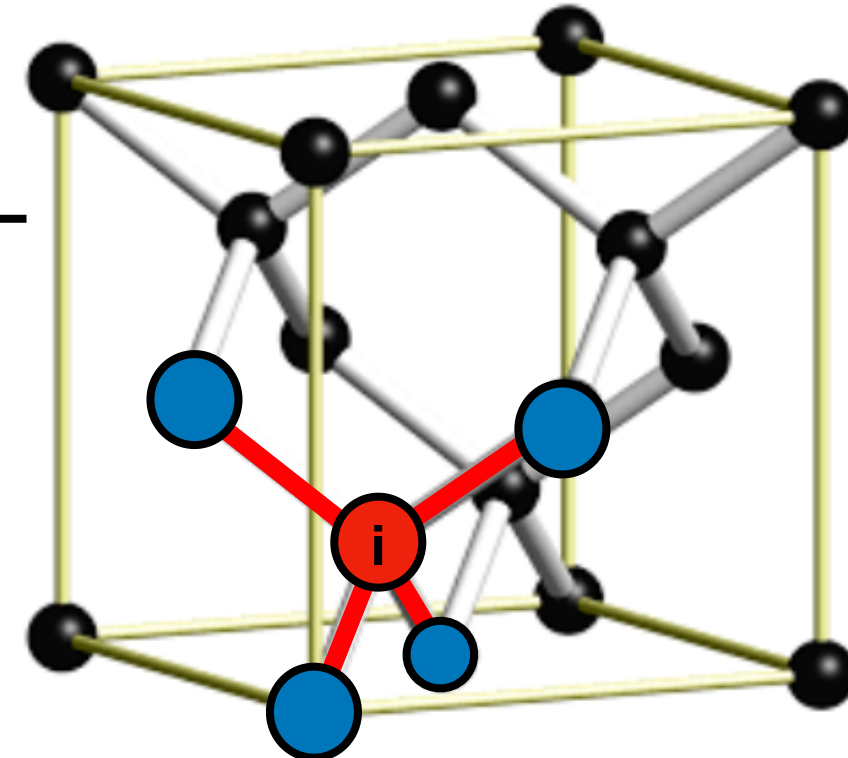
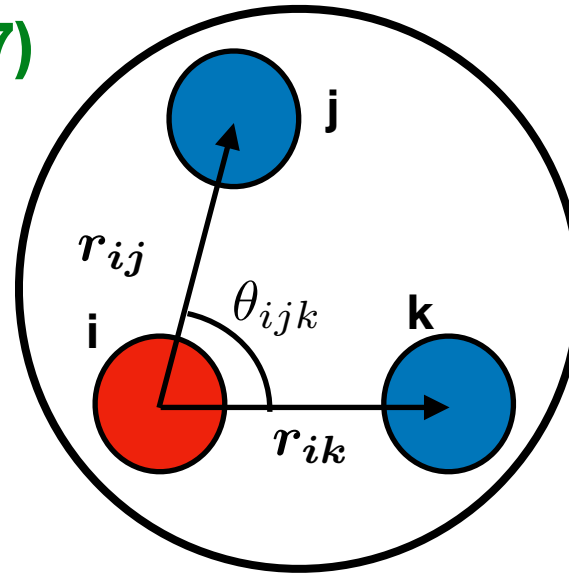
Cons

- Difficult to train/fit
 - requires intuition
- Hard to improve upon once finalized
- Accuracy limitations
- Slow relative to traditional potentials
- Bad extrapolation
- Slow relative to traditional potentials

PINN potential: Structure parameters

Structure parameters: (Mishin: 2017)

$$G_i^l = \sum_{j,k} P_l(\cos(\theta_{ijk})) f(r_{ij}) f(r_{ik})$$



Angular term:

$$P_l(\cos(\theta)) \quad l = 0, 1, 2, 4, 6$$

(Legendre polynomials)

Radial term:

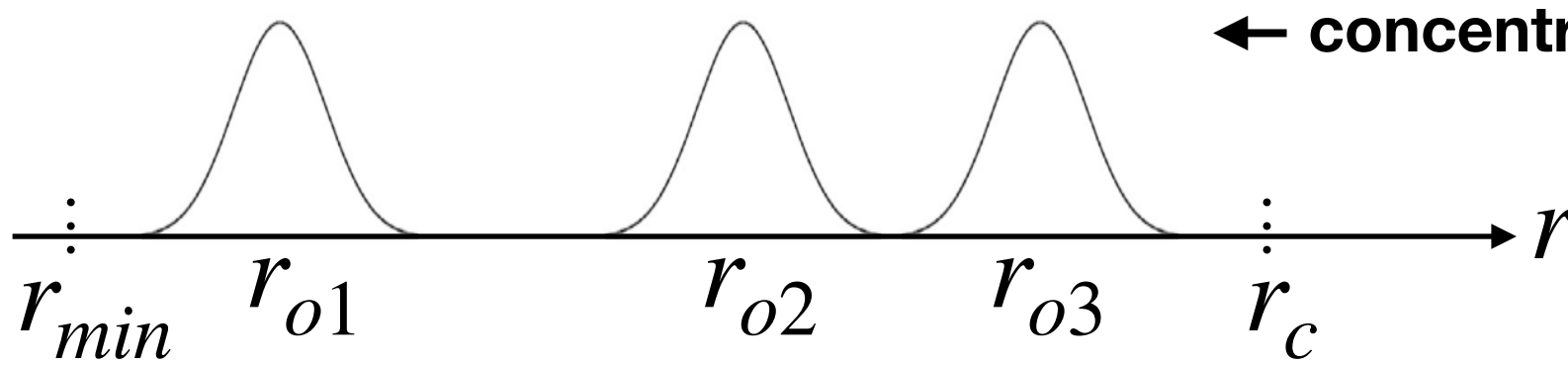
$$f(r) = \frac{1}{\sigma^3} e^{-\frac{(r-r_o)^2}{\sigma^2}} f_c(r)$$

choose multiple r_o values
(~8 to 12)

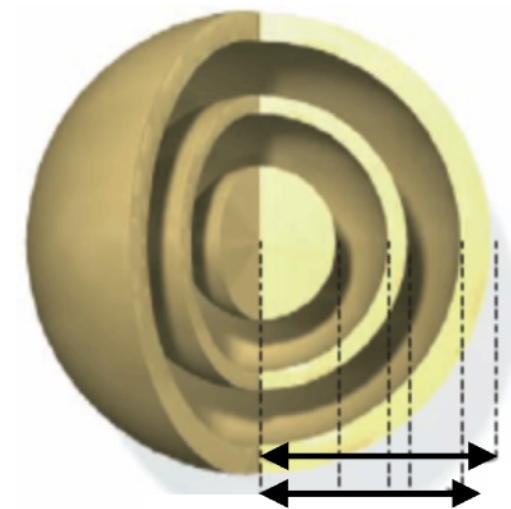
$f_c(r)$ = Cutoff function

**G_i 's act as
"fingerprints" of
the local atomic
environment**

$12 r_o$'s \rightarrow 60 G_i 's
per atom



← concentric shells →



PINN potential: BOP format (Mishin: 2017)

$$f_c(r) = \begin{cases} \frac{(r - r_c)^4}{d^4 + (r - r_c)^4} & r \leq r_c \\ 0, & r \geq r_c \end{cases}$$

cutoff function

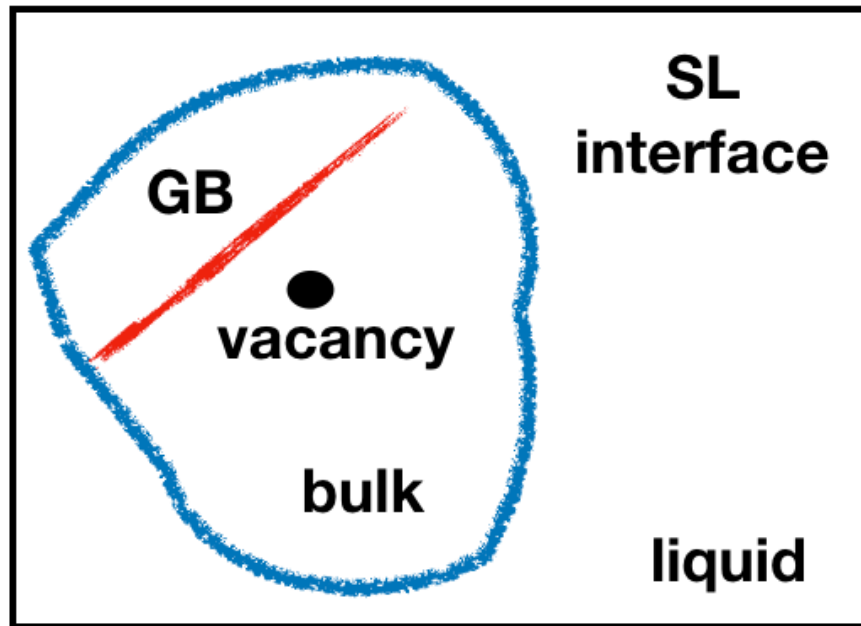
Note: r_c and d are fixed

$$E_i = \frac{1}{2} \sum_{j \neq i} \left[A_i e^{-\alpha_i r_{ij}} - B_i S_{ij} b_{ij} e^{-\beta_i r_{ij}} \right] f_c(r_{ij}) + E_i^{(p)}$$

(atom specific)

bond order parameter

promotion energy



$$b_{ij} = (1 + z_{ij})^{-1/2}$$

$$E_i^{(p)} = -\sigma_i \left(\sum_{j \neq i} S_{ij} b_{ij} f_c(r_{ij}) \right)^{1/2}$$

$$z_{ij} = \sum_{k \neq i, j} a_i S_{ik} (\cos \theta_{ijk} + h_i)^2 f_c(r_{ij}) \longleftrightarrow S_{ij} = \prod_{k \neq i, j} S_{ijk}$$

$$S_{ijk} = 1 - f_c(r_{ik} + r_{jk} - r_{ij}) e^{-\lambda_i (r_{ik} + r_{jk} - r_{ij})}$$

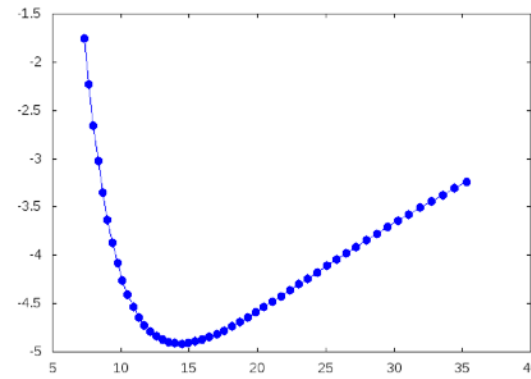
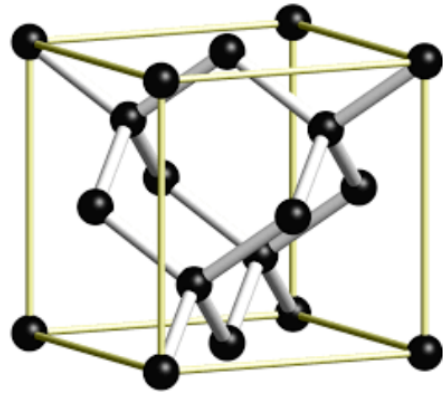
8 Adjustable parameter which are controlled by the outputs of the NN

$A_i, B_i, \alpha_i, \beta_i, a_i, h_i, \lambda_i$ and σ_i

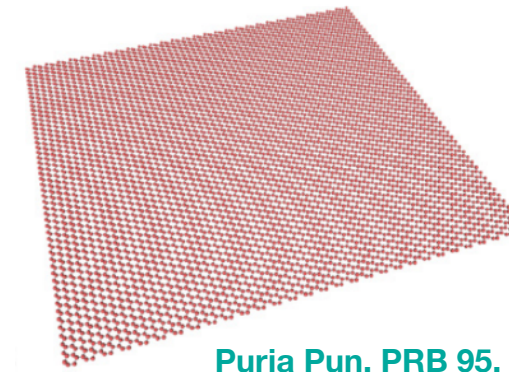
Silicon PINN potential (preliminary results)

Training/test set generation

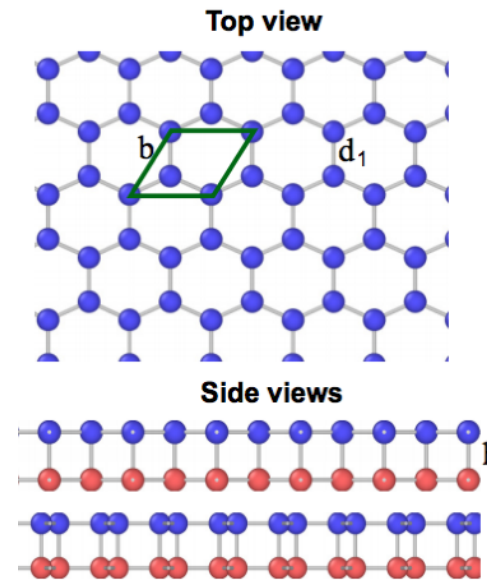
Stable structure:
(Diamond)



Two dimensional structures:

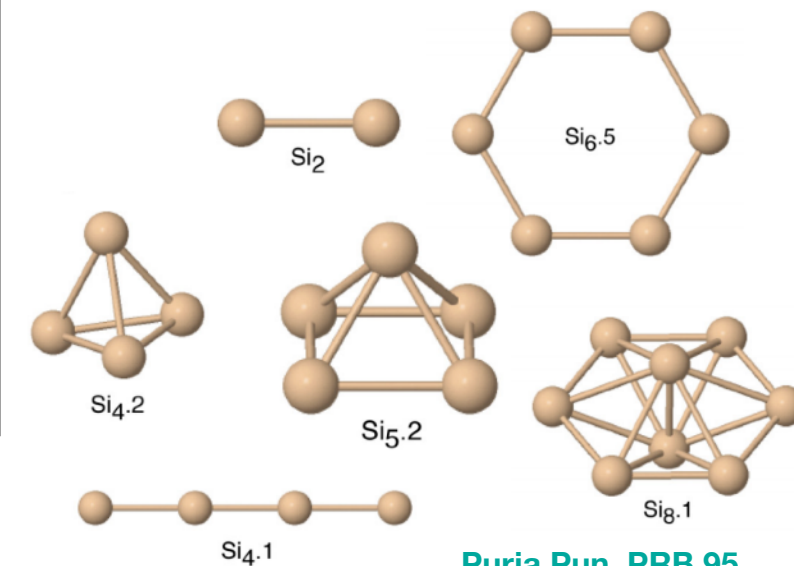


Purja Pun, PRB 95, 224103 (2017)



6 silicene allotropes

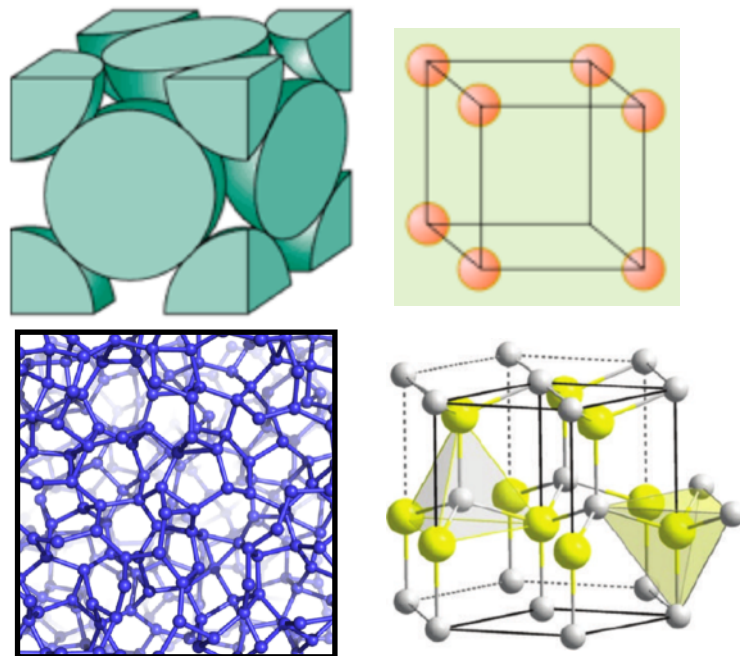
Clusters:



Purja Pun, PRB 95, 224103 (2017)

~18 atomic clusters

Alternative structures:



~14 alternate structures

- FCC, BCC, HEX, HCP, SC, Liquid, Amorphous ...etc

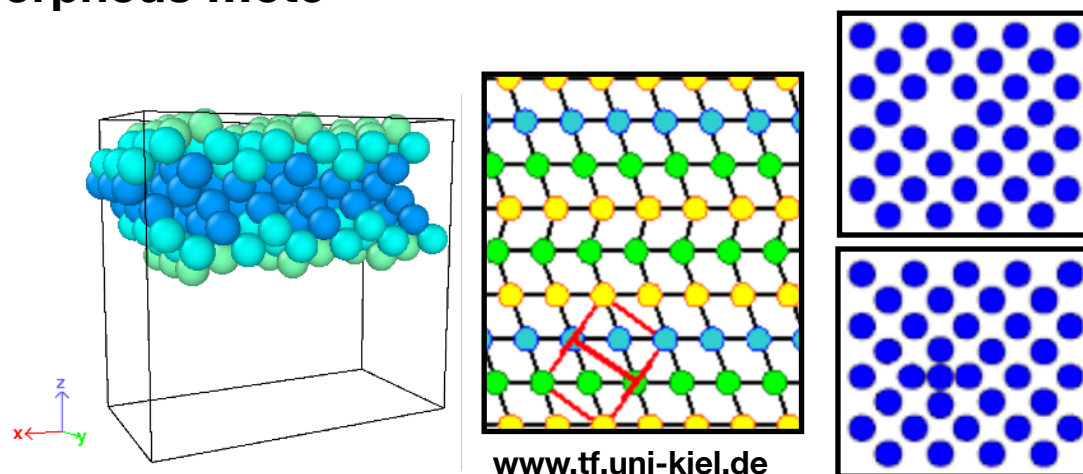
DFT calculation details

- Functional/PP: PBE/PAW
- ENCUT=600
- ~4300 structures
- block size 1-96 atoms
- k-point convergence tests for each group

Non-equilibrium sampling

- Isotropic expansions/compressions
- Random local atomic perturbations
- Anisotropic box variations

Defects:

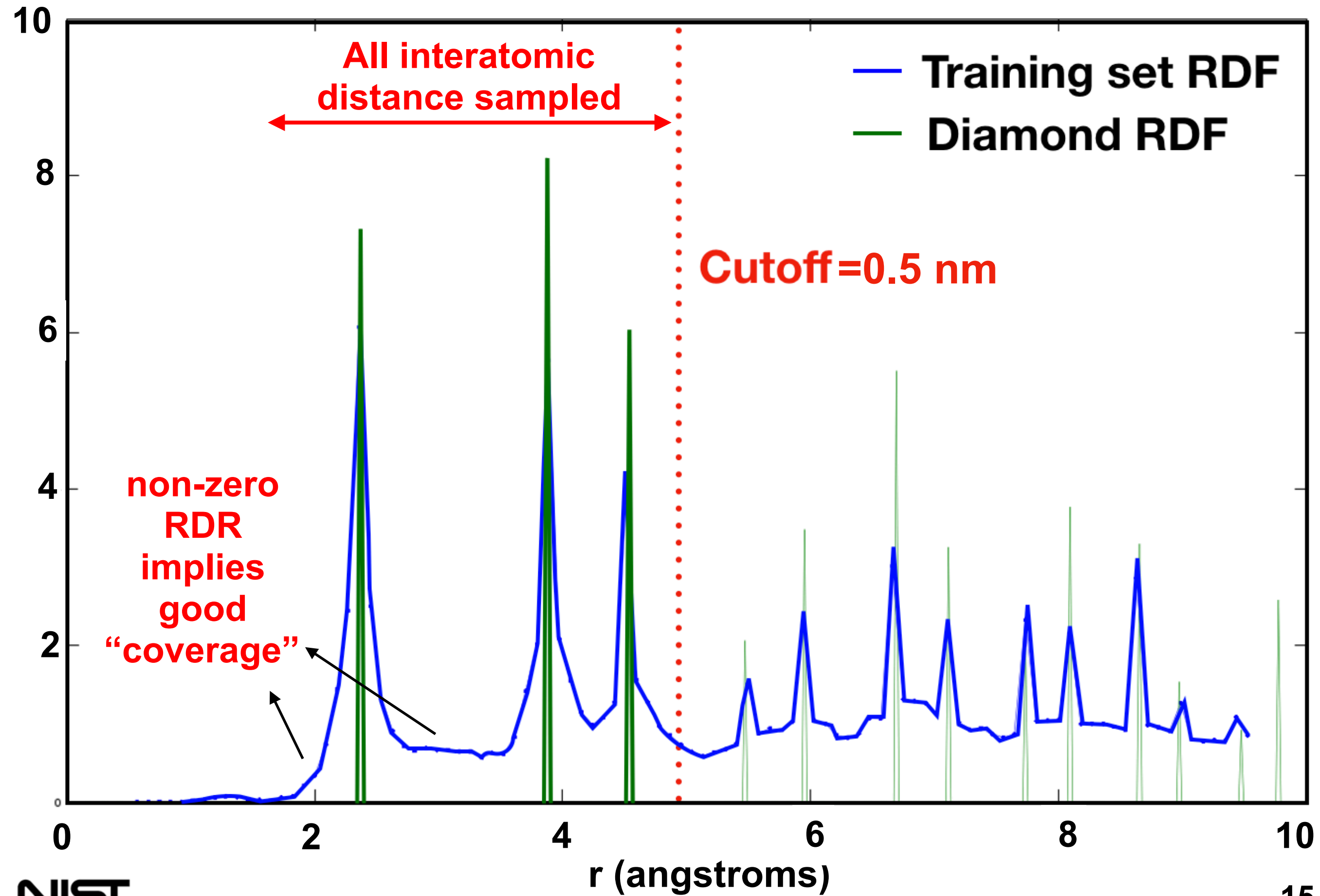


www.tf.uni-kiel.de

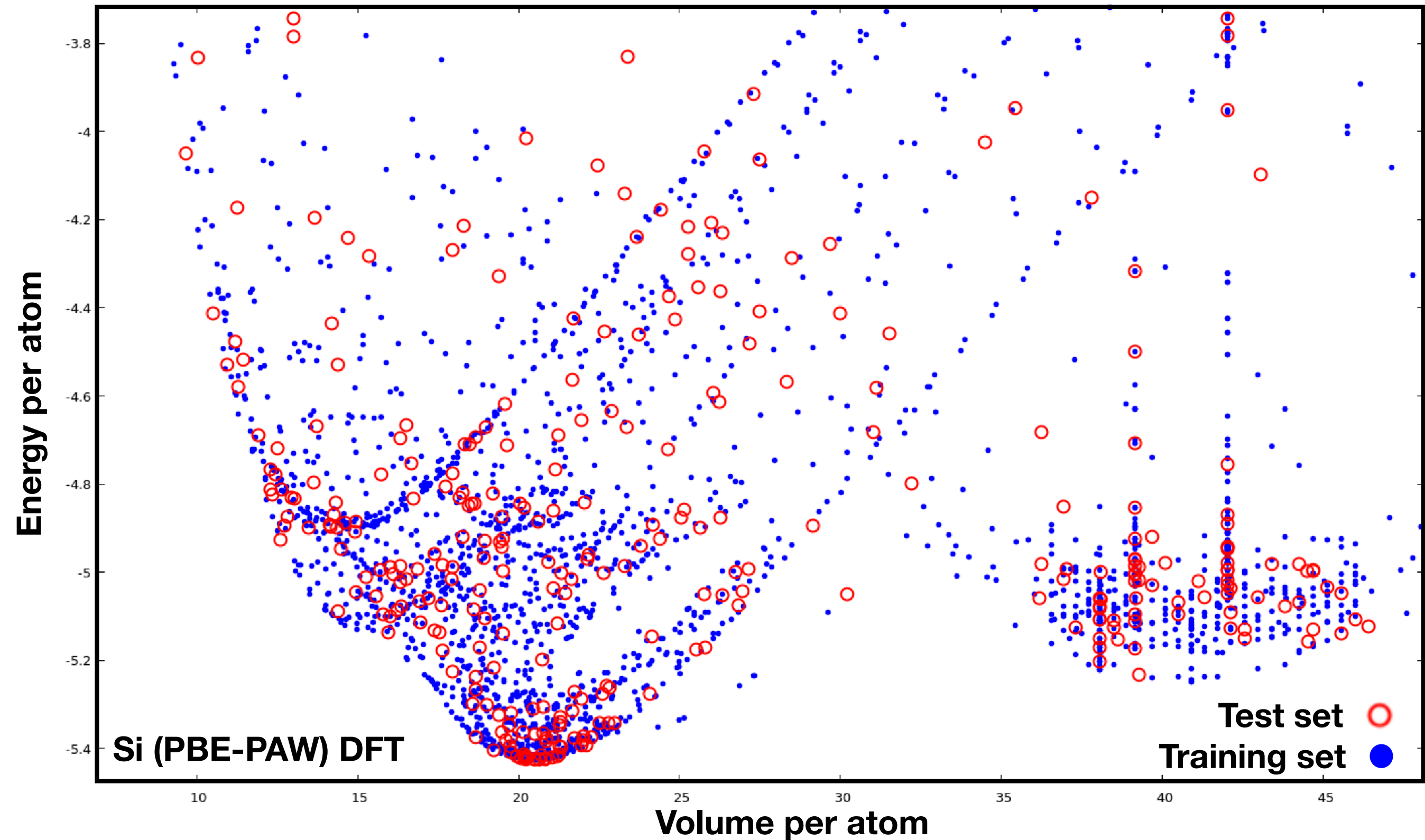
~27 different defects

- Vacancies, Various self interstitials, Surfaces, Stacking faults

Train set coverage



Training and test set



Full set = Test + Training = 110,000 atoms (4279 structures)
(random subsets) ↓ ↪ **95,000 atoms (3706 structures)**
15,000 atoms (575 structures)

Si PINN potential details

Methodological details:

12 uniformly spaced r_0 choices:

$r_0 = 1.25 \ 1.59 \ 1.92 \ 2.26 \ 2.60 \ 2.93$
 $3.27 \ 3.60 \ 3.94 \ 4.28 \ 4.61 \ 4.95$ \rightarrow **60 Gi's total**
 $\sigma = 0.1 \text{ nm}$

PINN:

16x16x8

Training set: (0.5 full set) (exploratory runs)

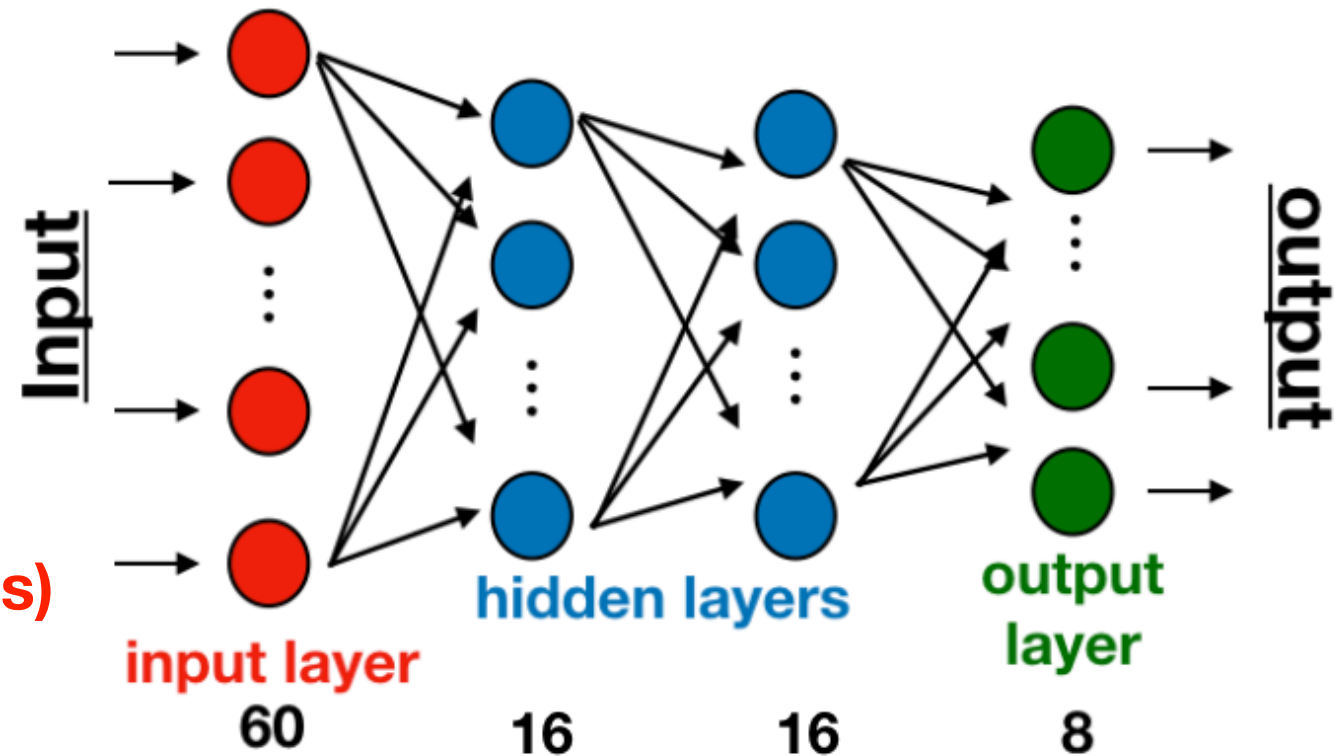
Number of structures: 1640

Total number of atoms: 42832

Test set:

Number of structures: 501

Total number of atoms: 12812



NN fitting parameters: 1384

Cutoff function $r_c = 0.5 \text{ nm}$
parameters (global) $d = 0.15 \text{ nm}$

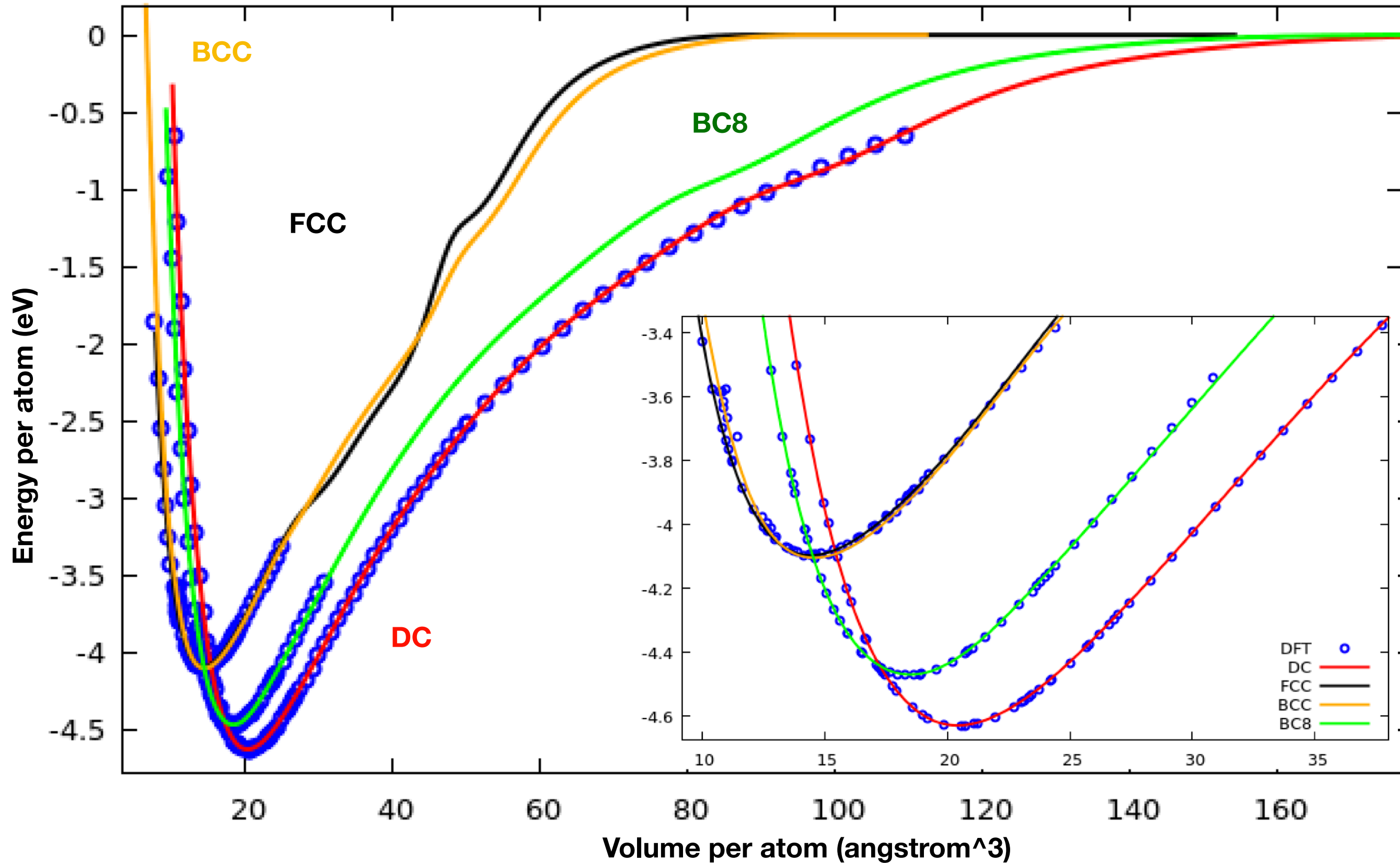
- DFT energy shifted by 0.79502 eV/atom \rightarrow DC=4.63 (eV/atom)

Start many NN's from different randomized IC, optimize and choose best

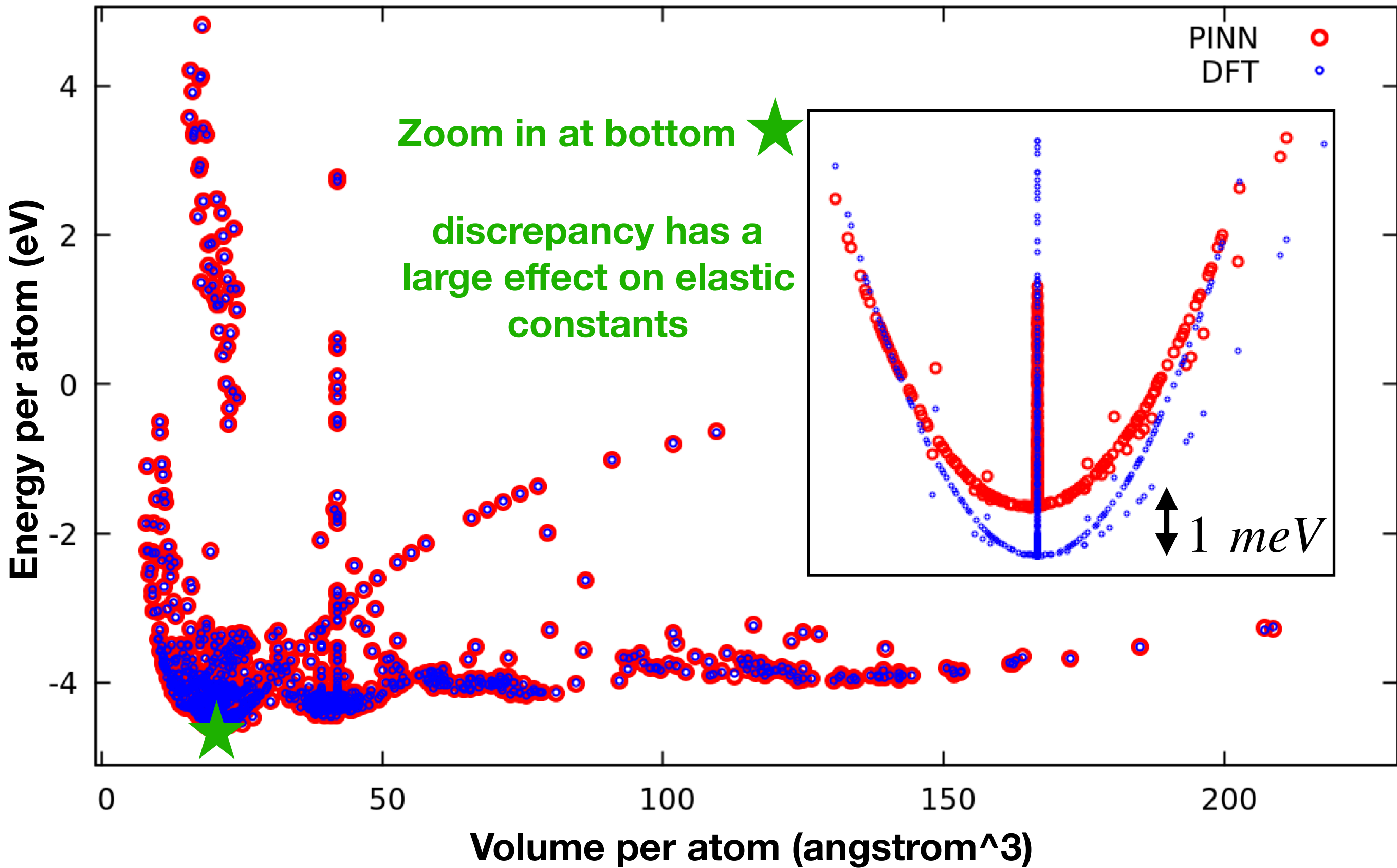
Fitting code reference: (“To be published”) [G. P. Purja Pun\(1\)](#), [R. Batra\(2\)](#), [R. Ramprasad \(3\)](#) and [Y. Mishin\(1\)](#)

(1) George Mason Univ., (2) Univ. Connecticut, (3) Georgia Tech

Select Si PINN potential equations of state

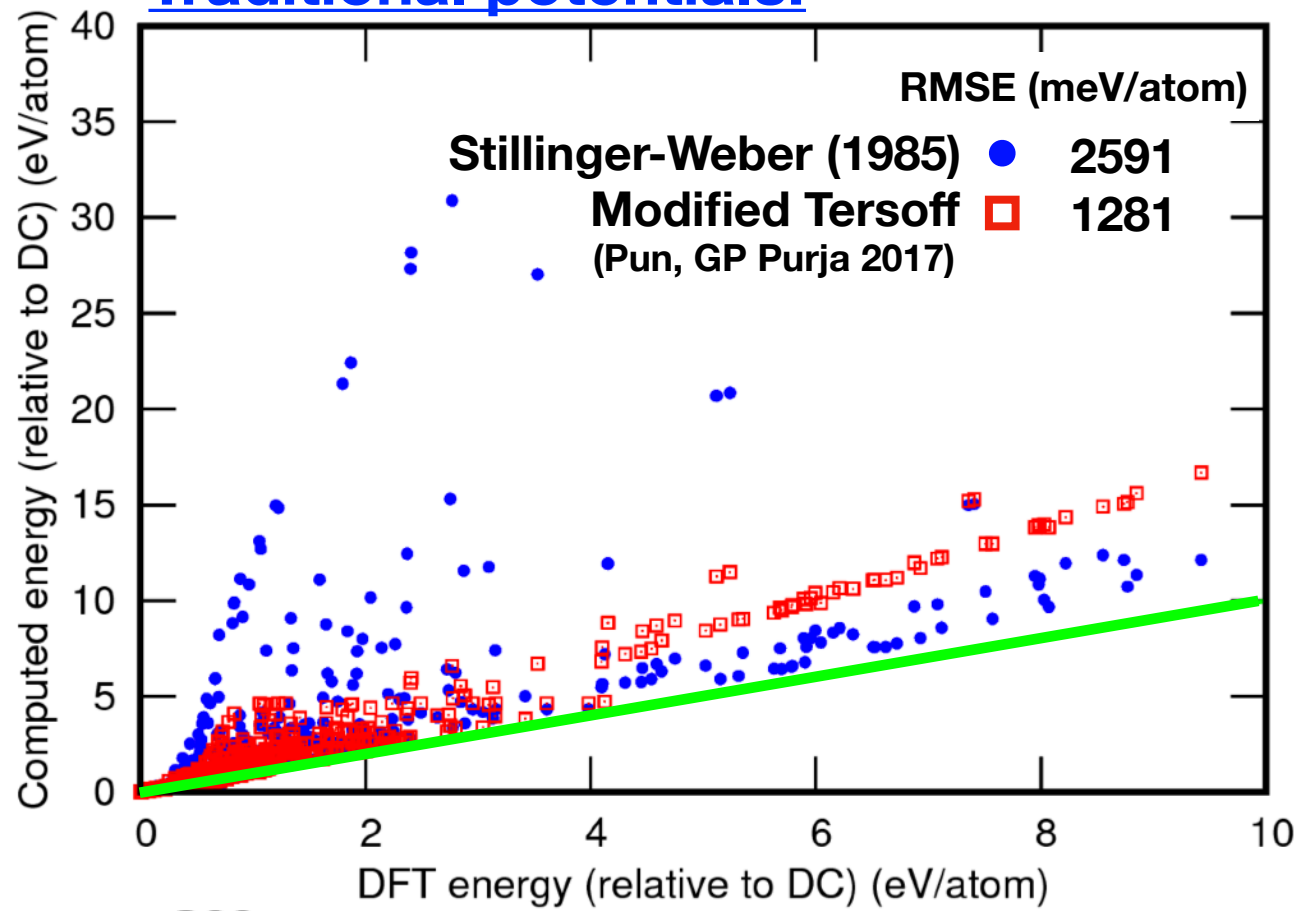


Results: Silicon PINN Potential

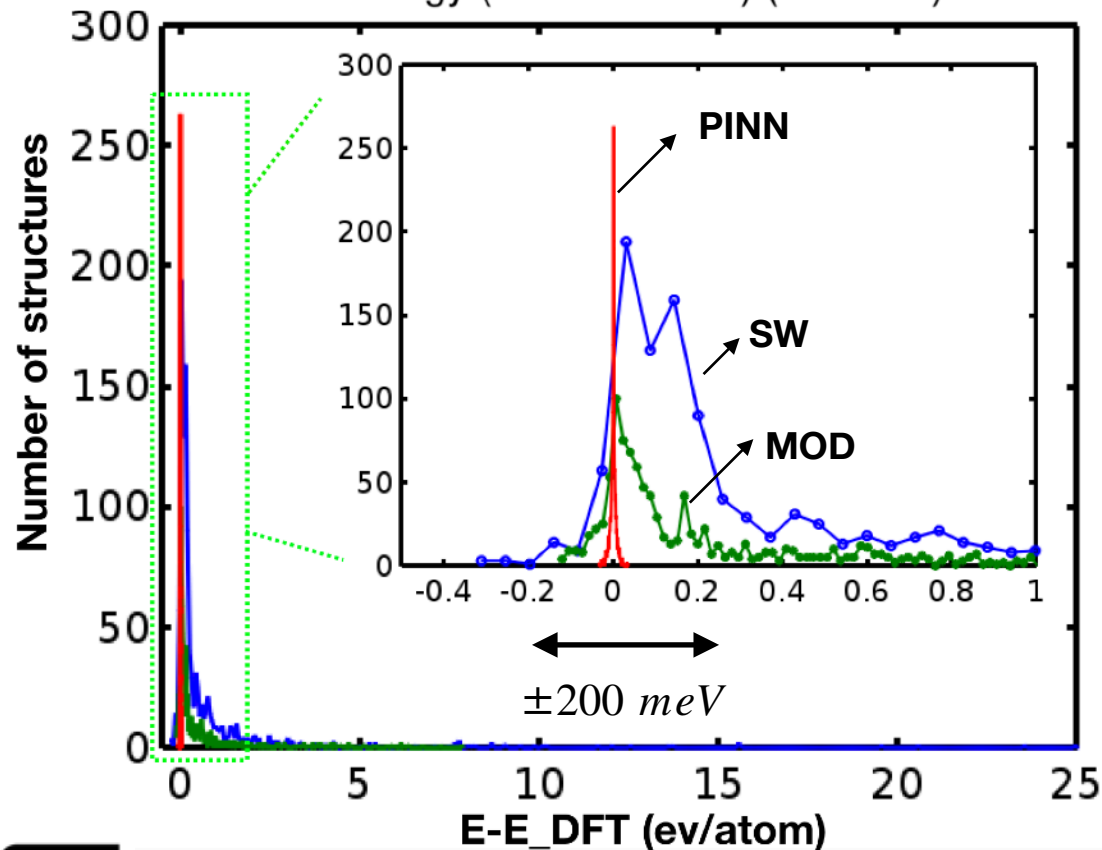
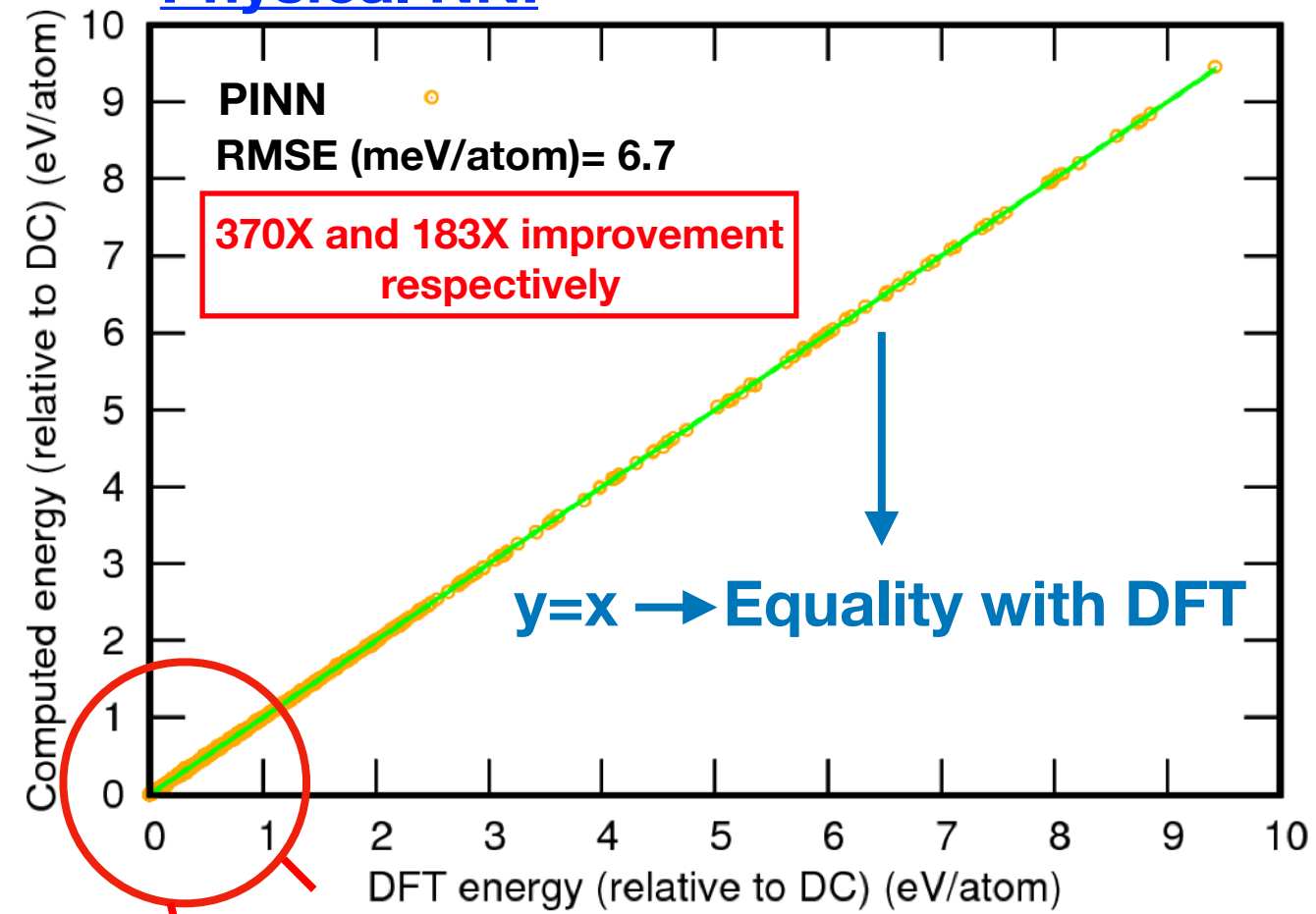


Si PINN comparison with traditional potential

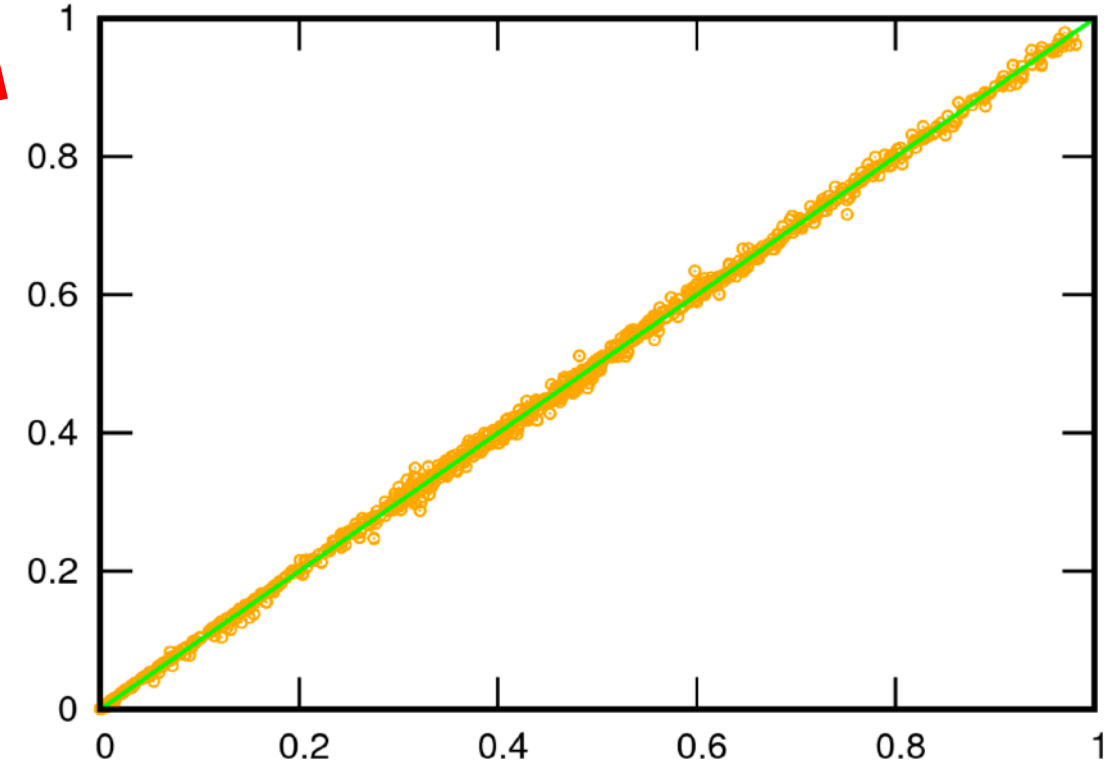
Traditional potentials:



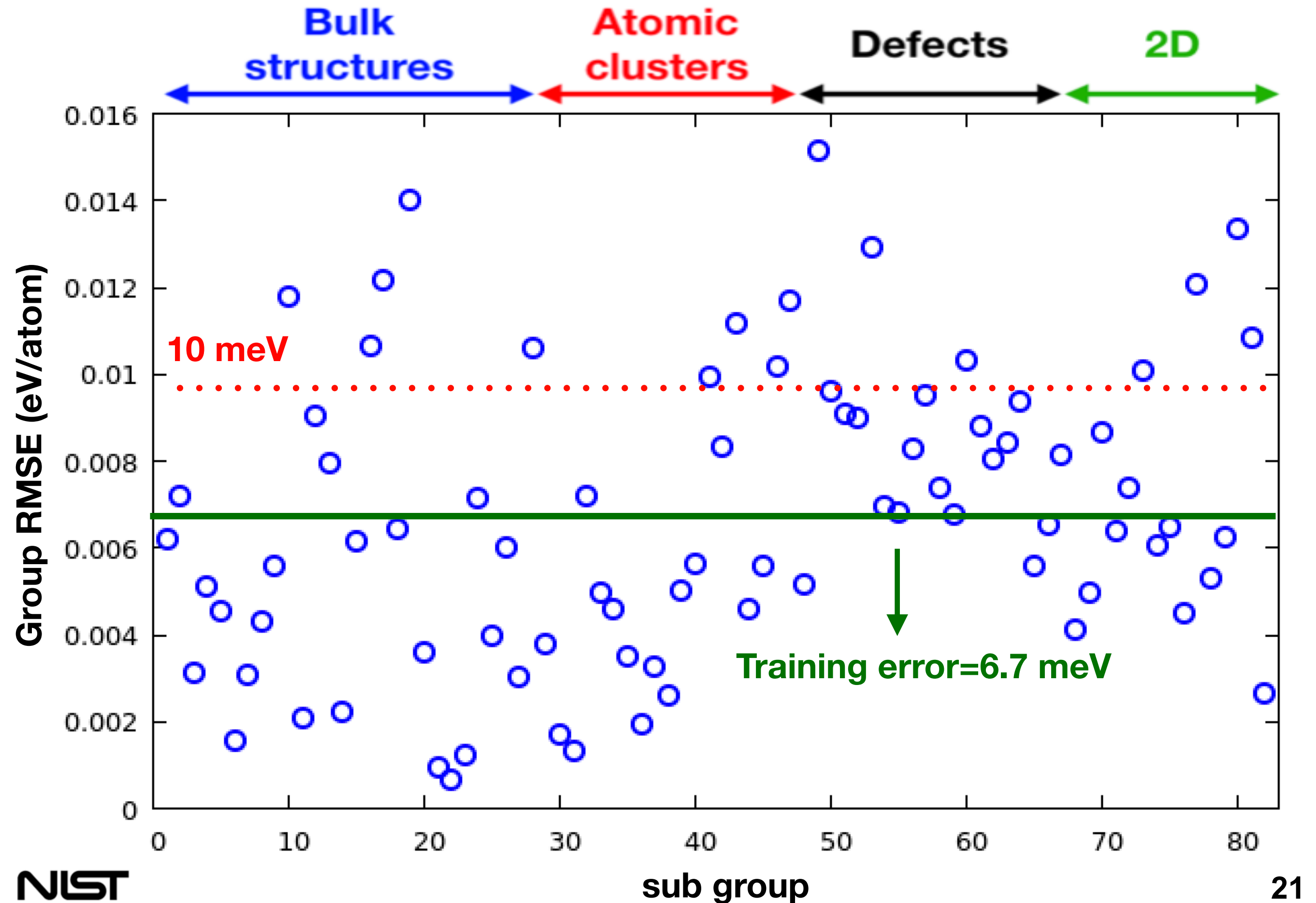
Physical NN:



zoom in



Si PINN subgroup RMSE



Aluminum

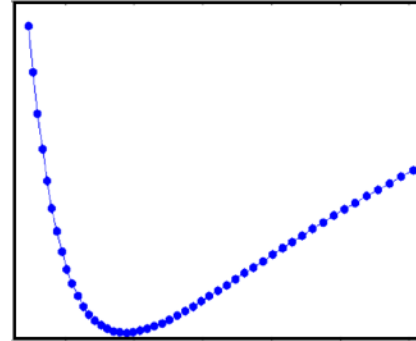
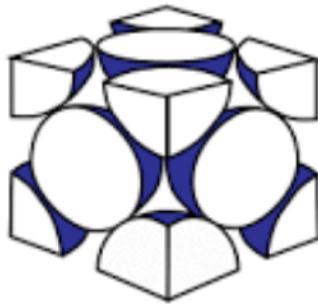
(“To be published”) G. P. Purja Pun(1), R. Batra(2), R. Ramprasad (3) and Y. Mishin(1)
(1) George Mason Univ., (2) Univ. Connecticut, (3) Georgia Tech

Aluminum NN and PINN Potential

Training/test set:

Stable Phase (ab-initio MD)

FCC ($a=3.75 \text{ \AA}$)
 FCC ($a=3.96 \text{ \AA}$)
 FCC ($a=4.0 \text{ \AA}$)
 FCC ($a=4.10 \text{ \AA}$)
 FCC ($a=4.15 \text{ \AA}$)
 FCC ($a=4.35 \text{ \AA}$)



T=700 K, 1200 K, 2500 K

expansion/compression

Database source:

V. Botu, R. Batra, J. Chapman, and R. Ramprasad. Machine learning force fields: Construction, validation, and outlook. *The Journal of Physical Chemistry C*, 121(1):511–522, 01 2017. URL: <https://doi.org/10.1021/acs.jpcc.6b10908>, doi:10.1021/acs.jpcc.6b10908.

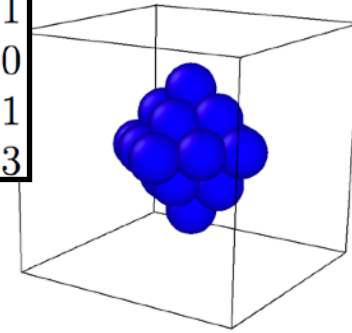
Alternate structures (0K)

FCC	isotropic strain at 0K
BCC	isotropic strain at 0K
HCP	isotropic strain at 0K
SC	isotropic strain at 0K
DC	isotropic strain at 0K
FCC	uniaxial $\langle 100 \rangle$ at 0K
A15*	isotropic strain at 0K
HEX*	isotropic strain at 0K
FCC*	uniaxial $\langle 100 \rangle$ at 0K
FCC*	uniaxial $\langle 111 \rangle$ at 0K

Clusters+Defects (ab-initio MD)

GB 111	Surface 100
GB 210	Surface 110
GB 310	Surface 111
GB 320	Surface 200
GB 510	Surface 311
SF $\langle 211 \rangle, (111)$	Surface 333

1 Vac
1 adatom on (100)
2 adatoms on (111)
Dimer adatom on (111)
Trimer adatom on (111)



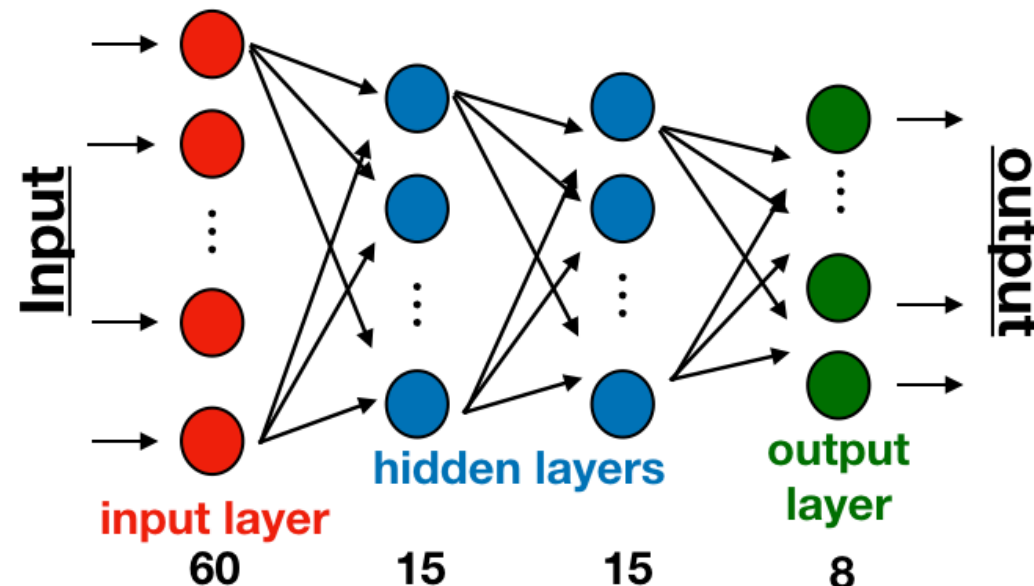
Full set=Test+Training=127,592 atoms (3649 structures)
 (random subsets) ↓ ↪ 108,052 atoms (3154 structures)
 19,540 atoms (495 structures)

Methodological details:

- Both straight and physical NN
- DFT energy shifted by 0.38446 eV/atom

PINN:

15×15×8



Fit	Size	N_P	N_{Gi}	N_{r0}
NN	16×16×1	1265	5	12
Physical NN	15×15×8	1283	5	12

NN fitting parameters

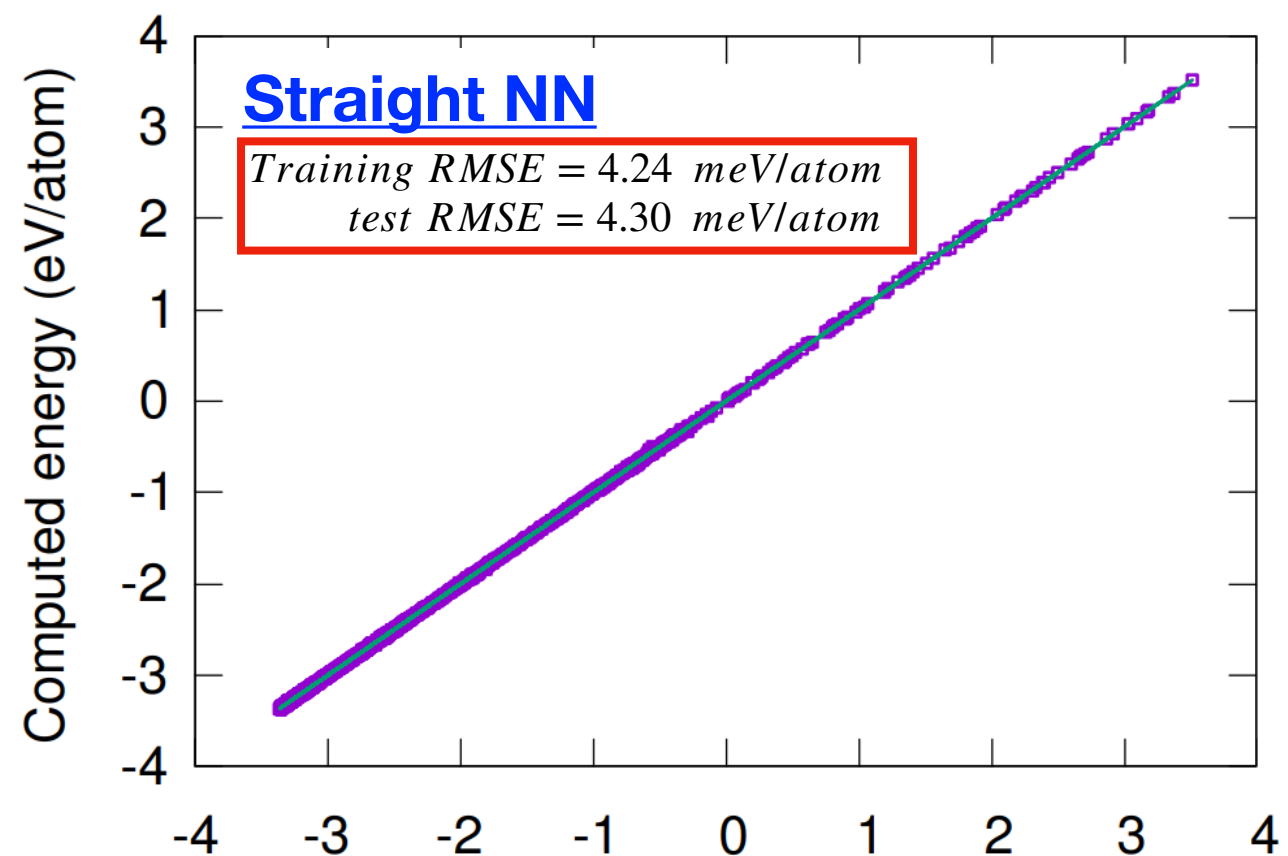
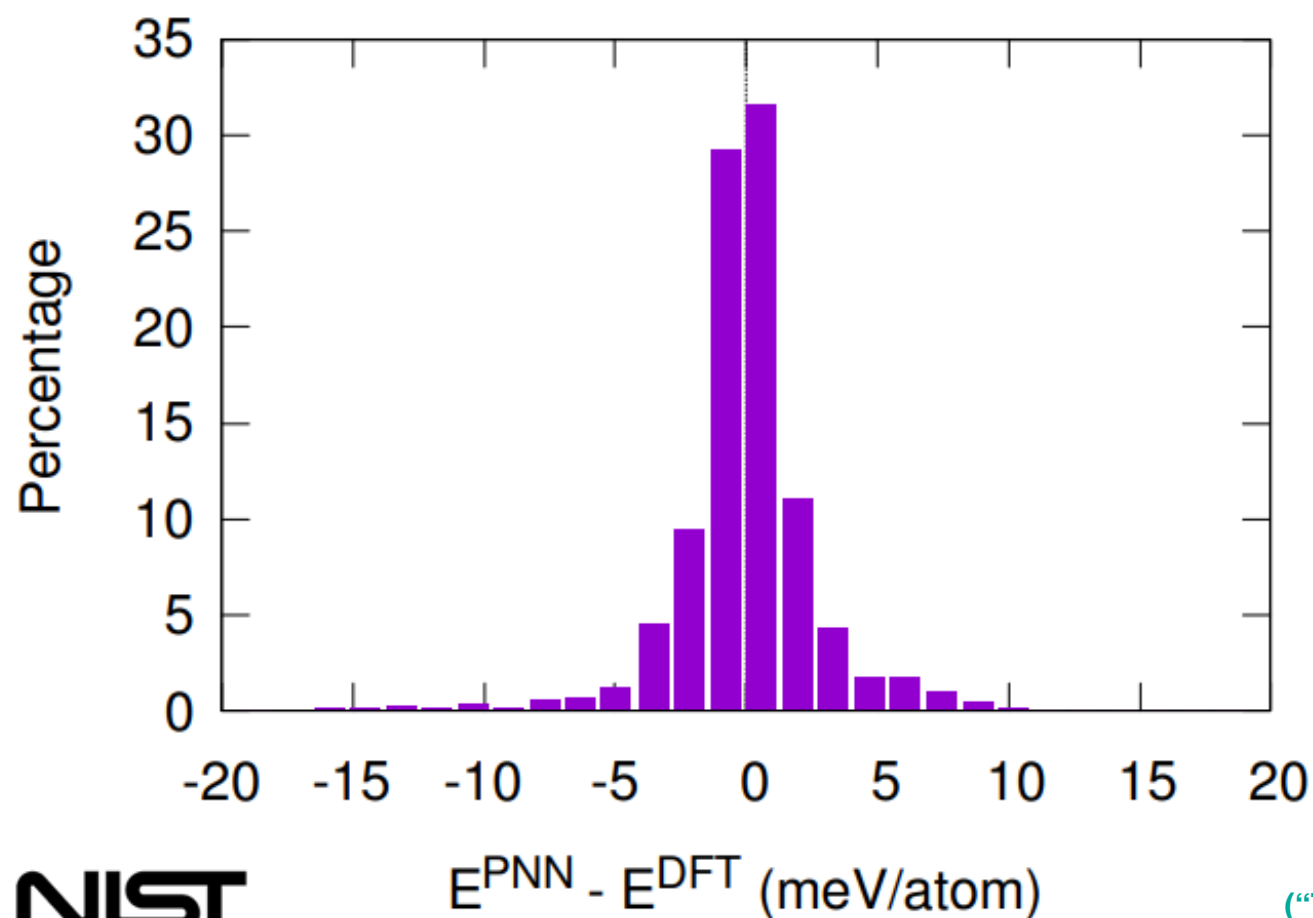
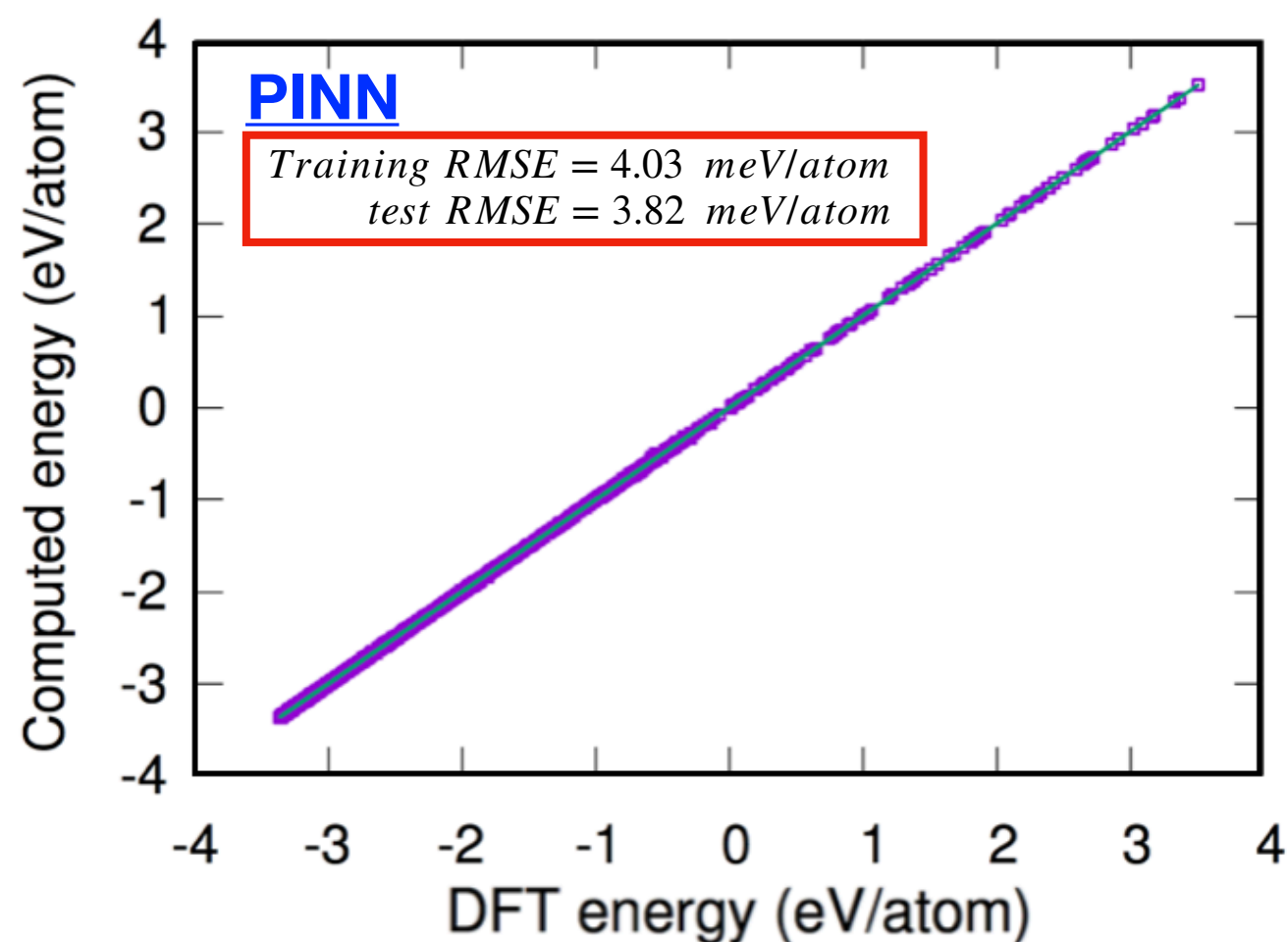
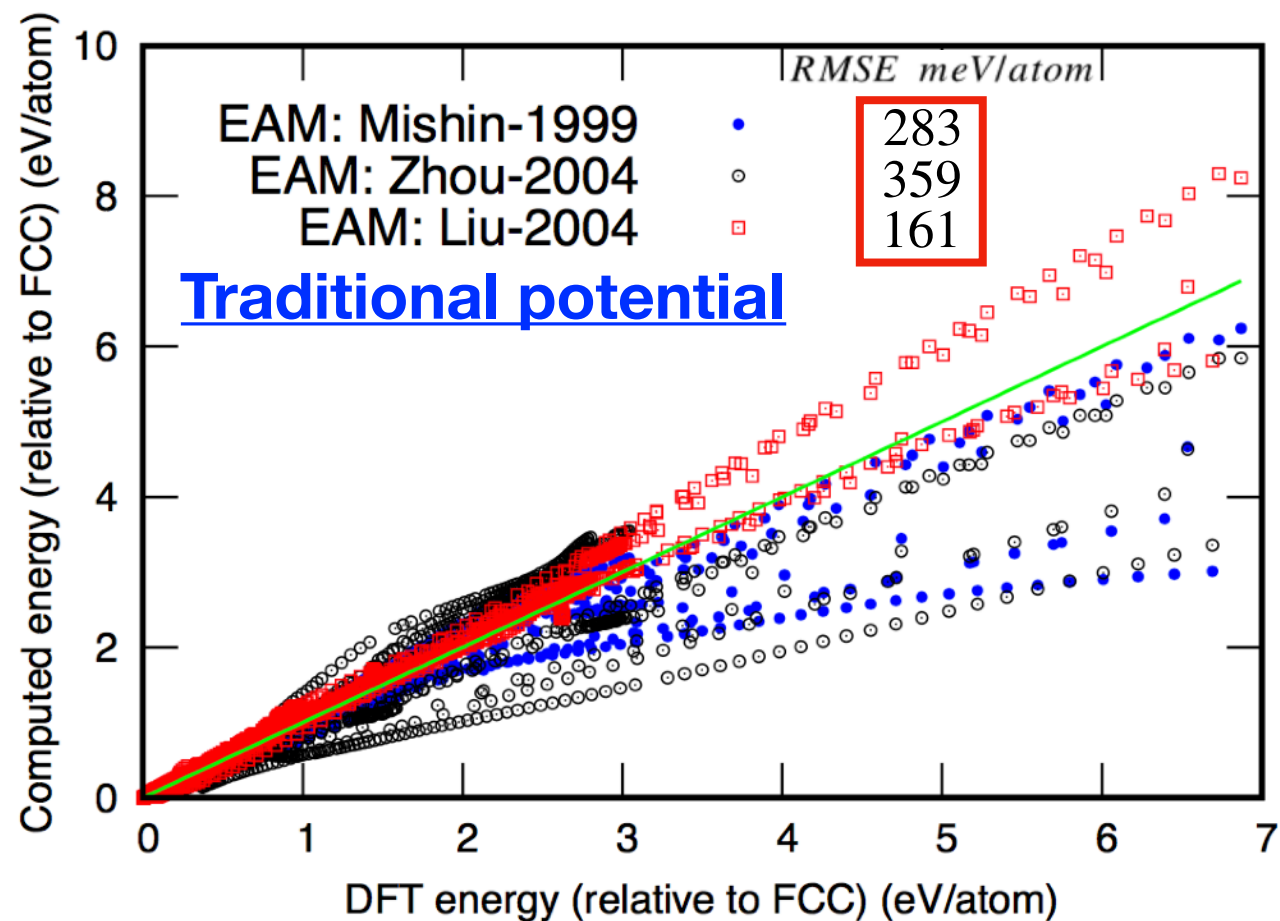
Cutoff function parameters (global)

$$r_c = 0.6 \text{ nm}$$

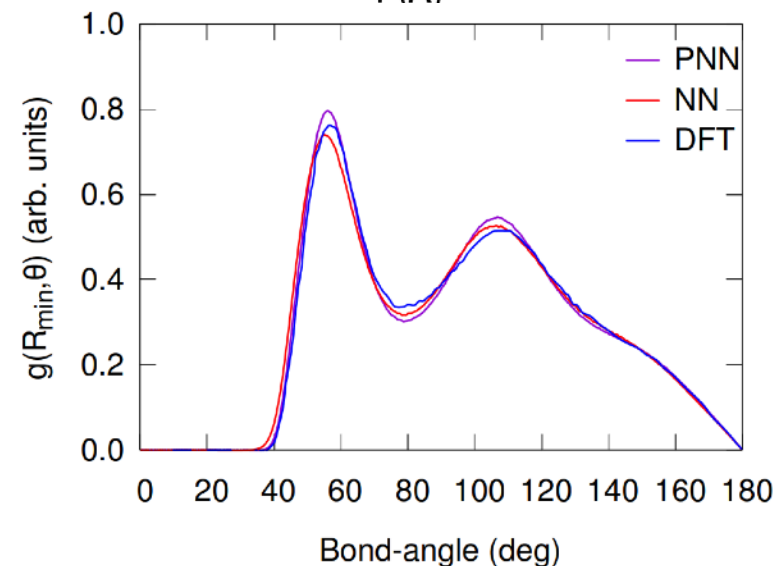
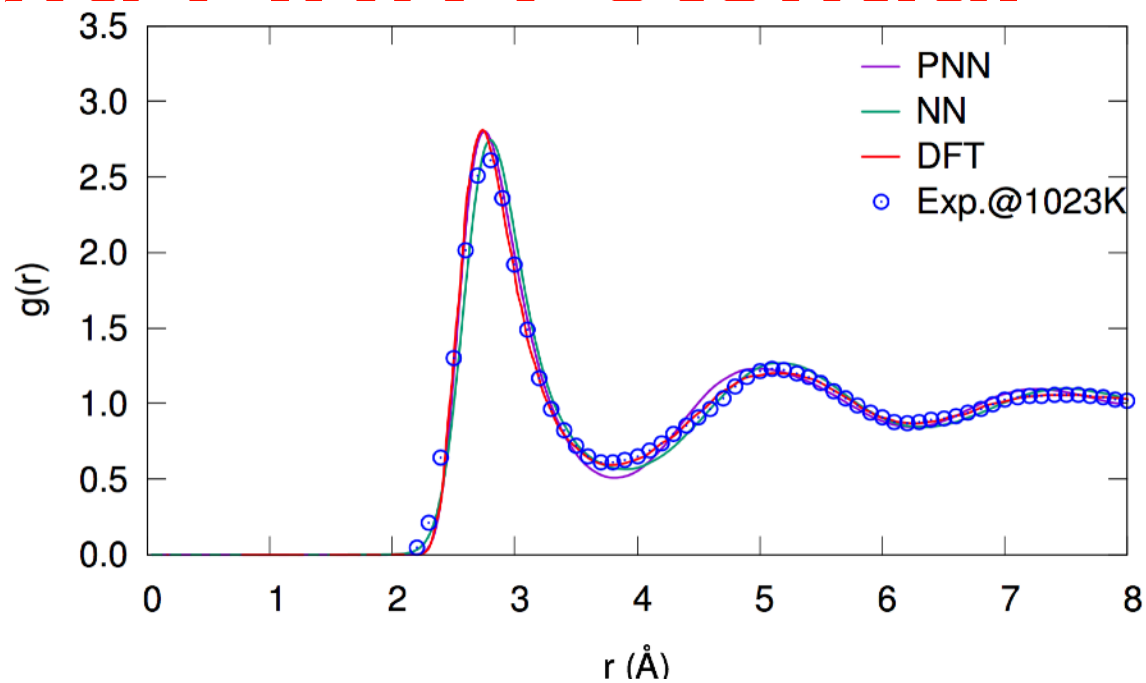
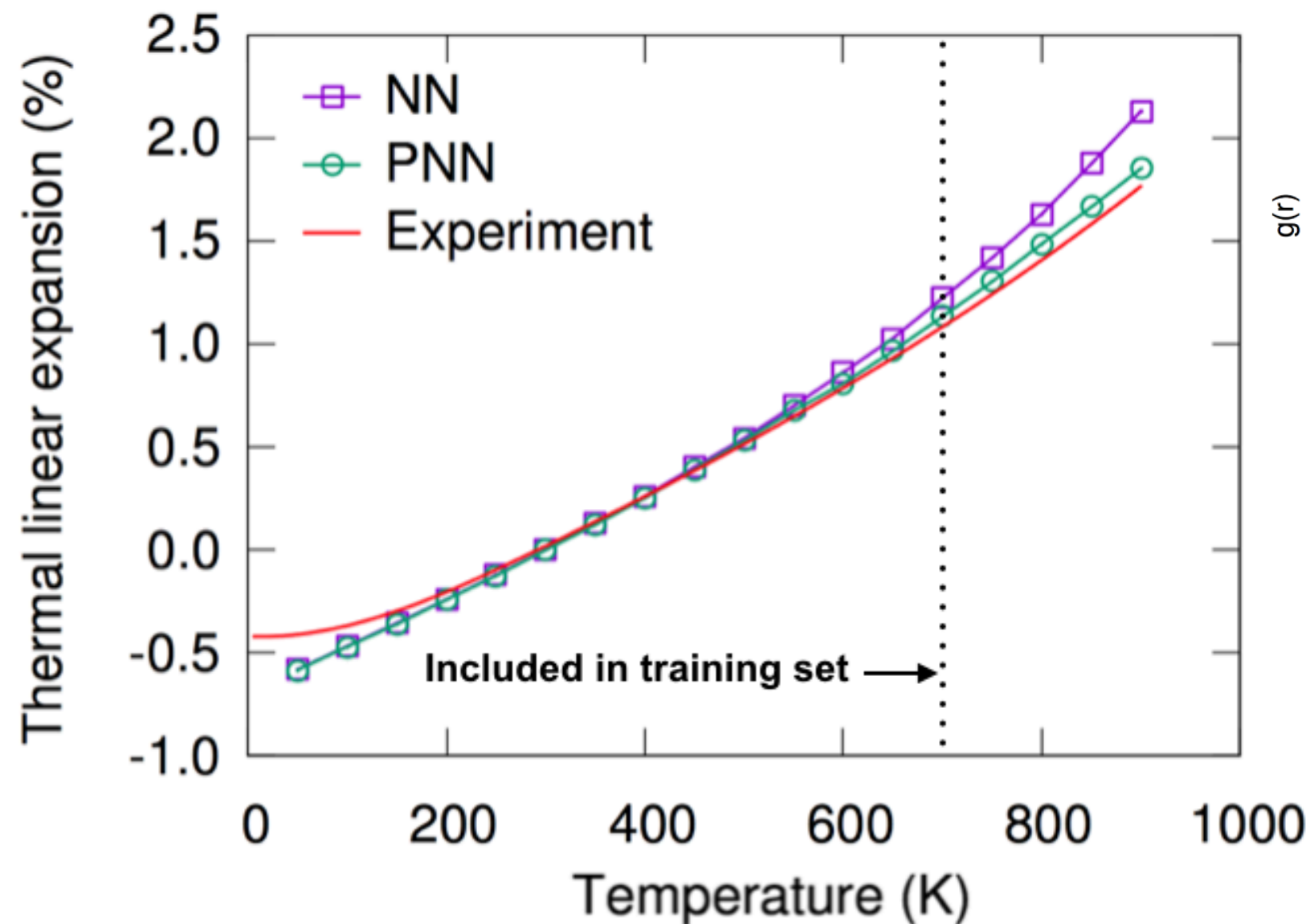
$$d = 0.15 \text{ nm}$$

60 Gi's total

Results: Aluminum NN and PINN Potential



Results: Aluminum NN and PINN Potential



Additional Properties:

Property	Ab initio	NN	Physical NN
E_0 (eV/atom)	3.7480 ^a	-3.3609	-3.3611
a_0 (Å)	4.039 ^{a,d} ; 3.9725–4.0676 ^c	4.0431	4.0398
B (GPa)	83 ^a ; 81 ^f	79	81
c_{11} (GPa)	104 ^a ; 103–106 ^d	109	118
c_{12} (GPa)	73 ^a ; 57–66 ^d	65	62
c_{44} (GPa)	32 ^a ; 28–33 ^d	26	30
$\gamma_s(100)$ (Jm ⁻²)	0.92 ^b	0.8974	0.9047
$\gamma_s(110)$ (Jm ⁻²)	0.98 ^b	1.0089	0.9644
$\gamma_s(111)$ (Jm ⁻²)	0.80 ^b	0.8471	0.8238

Property	Ab initio	NN	Physical NN
E_v^f (eV)	0.6646–1.3458 ^c ; 0.7 ^e	0.6558	0.7120
E_v^f (eV) unrelaxed	0.78 ^e	0.7412	0.7830
E_I^f (T_d) (eV)	2.2001–3.2941 ^c	2.7105	2.9133
E_I^f (O_h) (eV)	2.5313–2.9485 ^c	2.1573	2.5480
E_I^f $\langle 100 \rangle$ (eV)	2.2953–2.6073 ^c	1.8189	2.0558
E_I^f $\langle 110 \rangle$ (eV)	2.5432–2.9809 ^c	2.7924	2.6725
E_I^f $\langle 111 \rangle$ (eV)	2.6793–3.1821 ^c	2.6073	2.8375
γ_{SF} (mJ/m ²)	145.67 ^g	122	130
γ_{us} (mJ/m ²)		130	140

Future work

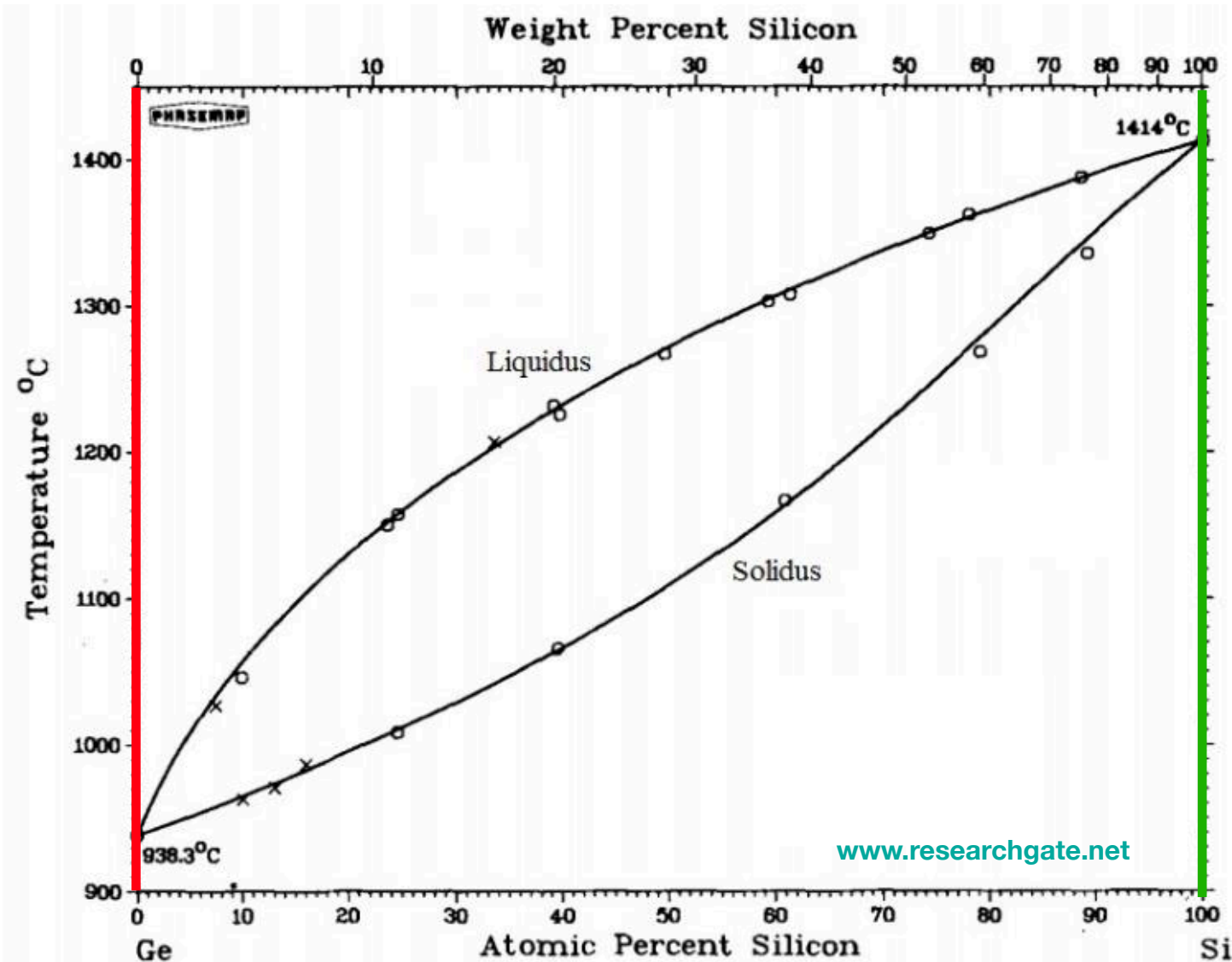
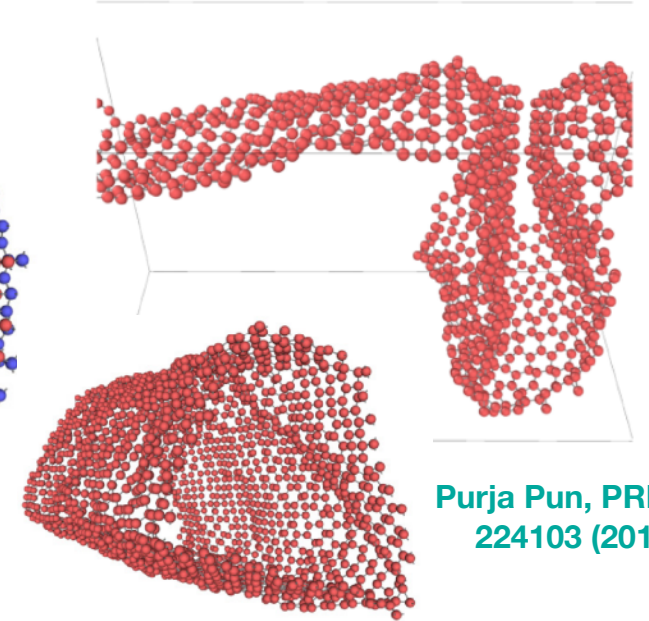
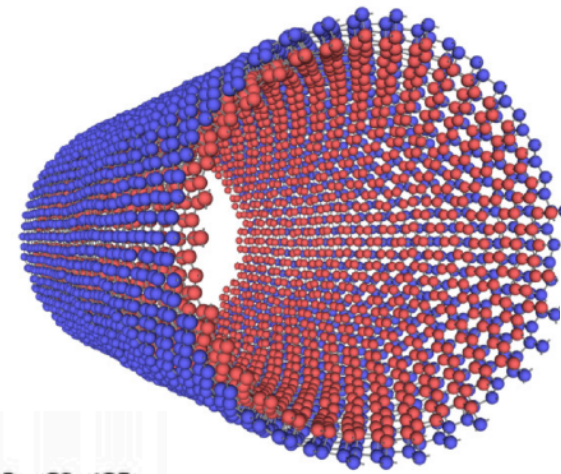
Future work-2

Germanium PINN potential:

2D Germanene stability

Germanene thermal conductivity

Binary SiGe PINN potential:



- Methodological:
 - leap frog
 - forward thinking
 - NN architecture
- Binary training set
- inheritance
- scalability

Ge PINN

Si PINN

Si-Ge PINN

Conclusions

- **Developed a new silicon interatomic potential using the new PINN potential format**
- **Even in preliminary stage we are obtaining excellent agreement with the DFT energies**
- **Current potential reproduces DFT data around 300x better than current traditional potentials**
- **Investigating methodological considerations to streamlining the fitting procedure for faster future development**

Acknowledgements

- Ganga Purja Pun
- Kamal Choudhary
- Vesselin Yamakov
- Francesca Tavazza
- Yuri Mishin
- GMU, NRC, NIST

NIST
National Institute of
Standards and Technology
U.S. Department of Commerce



**GEORGE
MASON
UNIVERSITY**

Image sources:

- https://www.tf.uni-kiel.de/matwis/amat/iss/kap_5/backbone/r5_3_3.html
- <https://www.wordstream.com/blog/ws/2017/07/28/machine-learning-applications>
- https://www.researchgate.net/figure/268158499_fig1_Figure-1-Phase-diagram-of-SiGe-alloys-showing-separation-of-the-solidus-and-liquidus
- <http://evolution.skf.com/us/bearing-research-going-to-the-atomic-scale>
- [/https://www.chegg.com/homework-help/questions-and-answers/consider-concentric-metal-sphere-spherical-shells-shown-figure--innermost-solid-sphere-rad-q4808250](https://www.chegg.com/homework-help/questions-and-answers/consider-concentric-metal-sphere-spherical-shells-shown-figure--innermost-solid-sphere-rad-q4808250)

Stillinger, Frank H., and Thomas A. Weber. "Computer simulation of local order in condensed phases of silicon." *Physical review B* 31.8 (1985): 5262.

("To be published") G. P. Purja Pun(1), R. Batra(2), R. Ramprasad (3) and Y. Mishin(1): (1) George Mason Univ., (2) Univ. Connecticut, (3) Georgia Tech

Pun, GP Purja, and Y. Mishin. "Optimized interatomic potential for silicon and its application to thermal stability of silicene." *Physical Review B* 95.22 (2017): 224103.

Extra Slides

Si PINN comparison with of properties

Properties:

```

Total number of clusters: 210
Check total number of configurations: 1640
Check total RMSError: 0.007201
deformation = 0.99976546
equil. energy of diam structure = -4.62903632 (eV/atom)
equil. volume of diam structure = 20.429451 (A^3/atom)
energy of (100) surface = 2.183343 (J/m^2)
energy of (110) surface = 1.776560 (J/m^2)
energy of (111) surface = 1.314244 (J/m^2)
vacancy formation energy = 3.20324940 (eV) (-4.62120403e+03)
Td interstitial formation energy = 4.013617 (eV)
<100> dumbbell formation energy = 8.435771 (eV)
<110> dumbbell formation energy = 23.287577 (eV)
HEX interstitial formation energy = 4.287206 (eV)
bond-center interstitial formation energy = 72.593833 (eV)
bulk modulus = 97.181035 (GPa)
c11 = 125.226780 (GPa)
shear modulus = 42.065657 (GPa)
c12 = 83.161123 (GPa)
c44 = 105.045461 (GPa)
EXECUTION TIME ON 32 CPU(S): 191.889600 s
    
```

Property	Experiment	DFT
E_c (eV/atom)	4.63 ^c	4.84 ^r
a (Å)	5.430 ^a	5.451 ^r
c_{11} (GPa)	165 ^a ; 167.40 ^b	
c_{12} (GPa)	64 ^a ; 65.23 ^b	
c_{44} (GPa)	79.2 ^a ; 79.57 ^b	
ν_{\max} (THz)	15.7 ^o	
Vacancy:		
$E_v^f(T_d)$ (eV)	3.6 ^j	3.17 ^m ; 3.69 ^t 3.29–4.3 ^h ; 3.70 – 3.84 ^s
$E_v^f(D_{3d})$ (eV)		3.97 ^t ; 4.29 ^v ; 4.37 ⁿ 3.67 – 3.70 ^s ; 5.023 ⁱ
Interstitials:		
E_i^f (hex) (eV)		3.31–5 ^h ; 2.87 – 3.80 ^s
$E_i^f(T_d)$ (eV)		3.43–6 ^h ; 3.43 – 5.10 ^s
$E_i^f(B)$ (eV)		4–5 ^h
$E_i^f\langle 110 \rangle$ (eV)		3.31–3.84 ^h ; 2.87 – 3.84 ^s
Surface energy γ_s (J m ⁻²):		
{111}	1.24 ^q ; 1.23 ^p	1.57 ^l ; 1.74 ^f
{100}		2.14 ^l ; 2.39 ^f ; 2.36 ^k
{100} _{2x1}	1.36 ^p	1.71 ^g ; 1.45 ^f ; 1.51 ^k
{110}	1.43 ^p	1.75 ^k
Melting:		
T_m (K)	1687	
$\Delta V_m / V_{\text{solid}}$ (%)	-5.1 ^a	
L (kJ/mol)	50.6 ^a	

Training and test set

1	A1	AMORPHOUS	UNPERTURBED+ISO	25	64	1600	1600
2	A2	AMORPHOUS	PERTURBED+ISO	65	64	4160	5760
3	B1	DC-P	UNPERTURBED+ISO	90	2	180	5940
4	B10	HCP-P	UNPERTURBED+ISO	70	2	140	6080
5	B11	DC-P	UNPERTURBED+UNIAXIAL+100	35	2	70	6150
6	B14	DC-C	UNPERTURBED+UNIAXIAL+111	25	48	1200	7350
7	B15	DC-C	PERTURBED+ISO	170	64	10880	18230
8	B17	SH-P-(HEX)	UNPERTURBED+ISO	70	1	70	18300
9	B2	DC-P	UNPERTURBED+FINE+ISO	80	2	160	18460
10	B20	Wurtzite-P	UNPERTURBED+ANISO	90	4	360	18820
11	B21	ST12-P	UNPERTURBED+ISO	70	12	840	19660
12	B23	FCC-P	PERTURBED+ISO	20	8	160	19820
13	B24	HCP-P	PERTURBED+ANISO	20	16	320	20140
14	B25	BCC-P	PERTURBED+ISO	20	8	160	20300
15	B26	SH-P-(HEX)	PERTURBED+ANISO	20	8	160	20460
16	B27	BSN-P	PERTURBED+ANISO	20	16	320	20780
17	B28	BC8-C	PERTURBED+ISO	5	128	640	21420
18	B29	Wurtzite-P	PERTURBED+ANISO	20	32	640	22060
19	B3	BCC-P	UNPERTURBED+ISO	90	1	90	22150
20	B30	ST12-P	PERTURBED+ANISO	10	96	960	23110
21	B31	DC-P	FINE-UNPERTURBED+SHEAR-2	250	2	500	23610
22	B32	DC-P	FINE-UNPERTURBED+100	250	2	500	24110
23	B33	DC-P	FINE-UNPERTURBED+SHEAR-1	250	2	500	24610
24	B4	SC-C	UNPERTURBED+ISO	90	1	90	24700
25	B5	BC8-C	UNPERTURBED+ISO	90	16	1440	26140
26	B6	BSN-P	UNPERTURBED+ISO	70	2	140	26280
27	B7	Wurtzite-P	UNPERTURBED+ISO	70	4	280	26560
28	B8	cP46-C	UNPERTURBED+ISO	50	46	2300	28860
29	B9	FCC-P	UNPERTURBED+ISO	90	1	90	28950
30	C11	Si5_2-PENTAMER-PYRAMID	UNPERTURBED+ISO	25	5	125	29075
31	C12	Si5_3-PENTAMER-BRIDGE	UNPERTURBED+ISO	25	5	125	29200
32	C13	Si5_4-PENTAMER-BIPYRAMID	UNPERTURBED+ISO	25	5	125	29325
33	C15	Si6_1-HEXAMER-CHAIR	UNPERTURBED+ISO	25	6	150	29475
34	C16	Si6_2-HEXAMER-OCTAHEDRON	UNPERTURBED+ISO	25	6	150	29625
35	C18	Si6_4-HEXAMER-FACECAP	UNPERTURBED+ISO	25	6	150	29775
36	C21	Si7_1-HEPTAMER-BI-PYRAMID	UNPERTURBED+ISO	25	7	175	29950
37	C22	Si8_1-OCTAMER-BI-PYRAMID	UNPERTURBED+ISO	25	8	200	30150
38	C6	Si4_2-TETRAMER-TD	UNPERTURBED+ISO	25	4	100	30250

Training and test set

39	C7	Si4_3-D4h-TETRAMER-SQUARE	UNPERTURBED+ISO	25	4	100	30350
40	C9	Si4_5-TETRAMER	UNPERTURBED+ISO	25	4	100	30450
41	D1	DC-C 1-VACANCY+PERTURBED+ISO	50	7	350	30800	
42	D10	DC-C 110-INTERSTITIAL+PERTURBED+ISO	50	9	450	31250	
43	D11	DC-C 2-VACANCY+PERTURBED+ISO	35	62	2170	33420	
44	D12	DC-C HEX-INTERSTITIAL+PERTURBED+ISO	35	65	2275	35695	
45	D13	DC-C Td-INTERSTITIAL+PERTURBED+ISO	35	65	2275	37970	
46	D14	DC-C B-INTERSTITIAL+PERTURBED+ISO	35	65	2275	40245	
47	D15	DC-C 110-INTERSTITIAL+PERTURBED+ISO	35	65	2275	42520	
48	D2	DC-C 1-VACANCY+PERTURBED+ISO	25	63	1575	44095	
49	D3	DC-C <-110><001>(110)+MESH	82	48	3936	48031	
50	D4	DC-C <010><001>(100)+MESH	116	32	3712	51743	
51	D5	DC-C <10-1><-12-1>(111)+MESH-GLIDE	106	96	10176	61919	
52	D6	DC-C <101><121>(111)+MESH-SHUFFLE	106	96	10176	72095	
53	D7	DC-C B-INTERSTITIAL+PERTURBED+ISO	50	9	450	72545	
54	D8	DC-C HEX-INTERSTITIAL+PERTURBED+ISO	50	9	450	72995	
55	D9	DC-C Td-INTERSTITIAL+PERTURBED+ISO	50	9	450	73445	
56	L2	LIQUID	PERTURBED+ISO	65	64	4160	77605
57	S1	SI-SURFACE-(100)-R	PERTURBED+ISO	35	16	560	78165
58	S10	SI-SURFACE-(320)	PERTURBED+ISO	35	40	1400	79565
59	S11	SI-SURFACE-(321)	PERTURBED+ISO	35	36	1260	80825
60	S12	SI-SURFACE-(322)	PERTURBED+ISO	35	36	1260	82085
61	S2	SI-SURFACE-(110)-R	PERTURBED+ISO	35	16	560	82645
62	S3	SI-SURFACE-(111)-R	PERTURBED+ISO	35	24	840	83485
63	S4	SI-SURFACE-(111)	PERTURBED+ISO	35	24	840	84325
64	S5	SI-SURFACE-(210)	PERTURBED+ISO	35	20	700	85025
65	S6	SI-SURFACE-(211)	PERTURBED+ISO	35	24	840	85865
66	S8	SI-SURFACE-(310)	PERTURBED+ISO	35	24	840	86705
67	S9	SI-SURFACE-(311)	PERTURBED+ISO	35	18	630	87335
68	T1	SILICENE-1-LAYER-HONEYCOMB	UNPERTURBED+ISO	25	18	450	87785
69	T10	SILICENE-PLANAR-BILAYER-AA_p	PERTURBED+ISO	45	36	1620	89405
70	T11	SILICENE-PLANAR-BILAYER-AA_p	PERTURBED+ANISO	25	36	900	90305
71	T13	SILICENE-BUCKLED-BILAYER-AA^p	PERTURBED+ISO	45	36	1620	91925
72	T14	SILICENE-BUCKLED-BILAYER-AA^p	PERTURBED+ANISO	25	36	900	92825
73	T15	SILICENE-BUCKLED-BILAYER-AB	UNPERTURBED+ISO	25	36	900	93725
74	T16	SILICENE-BUCKLED-BILAYER-AB	PERTURBED+ISO	45	36	1620	95345
75	T17	SILICENE-BUCKLED-BILAYER-AB	PERTURBED+ANISO	25	36	900	96245
76	T2	SILICENE-1-LAYER-HONEYCOMB	PERTURBED+ISO	45	18	810	97055
77	T3	SILICENE-1-LAYER-BUCKLED	UNPERTURBED+ISO	25	18	450	97505
78	T4	SILICENE-1-LAYER-BUCKLED	PERTURBED+ISO	45	18	810	98315
79	T5	SILICENE-1-LAYER-BUCKLED	PERTURBED+ANISO	25	18	450	98765
80	T7	SILICENE-1-LAYER-DUMBELL	PERTURBED+ISO	44	63	2772	101537
81	T8	SILICENE-1-LAYER-DUMBELL	PERTURBED+ANISO	25	63	1575	103112
82	T9	SILICENE-PLANAR-BILAYER-AA_p	UNPERTURBED+ISO	25	36	900	104012

Minimization algorithm

Davidon–Fletcher–Powell formula

From Wikipedia, the free encyclopedia

The **Davidon–Fletcher–Powell formula** (or **DFP**; named after [William C. Davidon](#), [Roger Fletcher](#), and [Michael J. D. Powell](#)) finds the solution to the secant equation that is closest to the current estimate and satisfies the curvature condition (see below). It was the first [quasi-Newton method](#) to generalize the [secant method](#) to a multidimensional problem. This update maintains the symmetry and positive definiteness of the [Hessian matrix](#).

Given a function $f(x)$, its [gradient](#) (∇f), and [positive-definite Hessian matrix](#) B , the [Taylor series](#) is

$$f(x_k + s_k) = f(x_k) + \nabla f(x_k)^T s_k + \frac{1}{2} s_k^T B s_k + \dots,$$

and the [Taylor series](#) of the gradient itself (secant equation)

$$\nabla f(x_k + s_k) = \nabla f(x_k) + B s_k + \dots$$

is used to update B .

The DFP formula finds a solution that is symmetric, positive-definite and closest to the current approximate value of B_k :

$$B_{k+1} = (I - \gamma_k y_k s_k^T) B_k (I - \gamma_k s_k y_k^T) + \gamma_k y_k y_k^T,$$

where

$$y_k = \nabla f(x_k + s_k) - \nabla f(x_k),$$
$$\gamma_k = \frac{1}{y_k^T s_k},$$

and B_k is a symmetric and [positive-definite matrix](#).

The corresponding update to the inverse Hessian approximation $H_k = B_k^{-1}$ is given by

$$H_{k+1} = H_k - \frac{H_k y_k y_k^T H_k}{y_k^T H_k y_k} + \frac{s_k s_k^T}{y_k^T s_k}.$$

B is assumed to be positive-definite, and the vectors s_k^T and y must satisfy the curvature condition

$$s_k^T y_k = s_k^T B s_k > 0.$$

The DFP formula is quite effective, but it was soon superseded by the [BFGS formula](#), which is its dual (interchanging the roles of y and s).

Elastic Constants

DFT PBE

Jarvis (ionic relaxation)

$$c_{11} = 152.7 \text{ GPa}$$

$$c_{12} = 57.0 \text{ GPa}$$

$$c_{44} = 74.4 \text{ GPa}$$

<https://www.ctcms.nist.gov/~knc6/jsmol/JVASP-1001.html>

Material Project (ionic relaxation)

$$c_{11} = 144.0 \text{ GPa}$$

$$c_{12} = 53.0 \text{ GPa}$$

$$c_{44} = 75 \text{ GPa}$$

<https://materialsproject.org/materials/mp-149/>

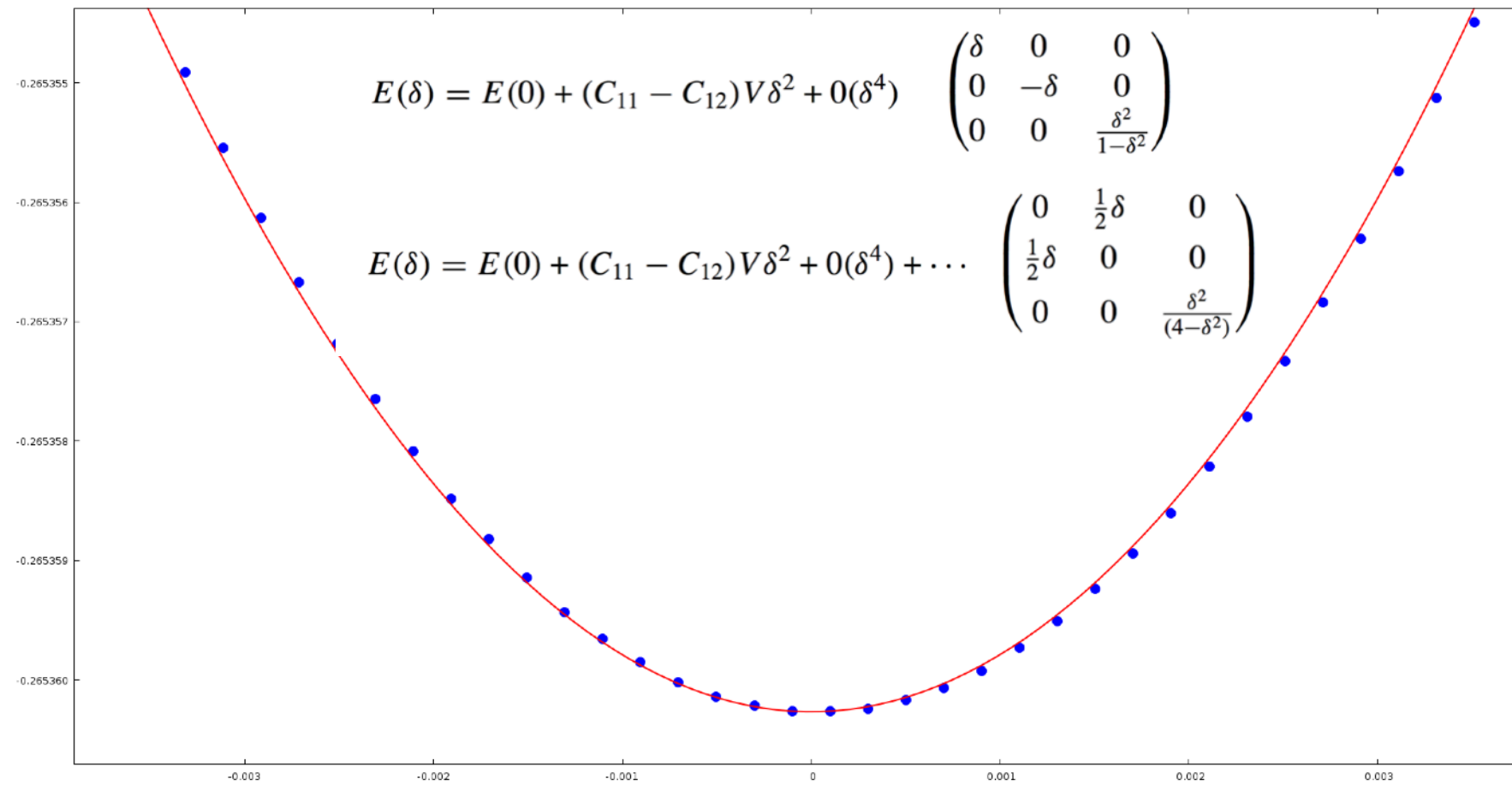
Current (no ionic relaxation)

$$c_{11} = 153.3 \text{ GPa}$$

$$c_{12} = 56.7 \text{ GPa}$$

$$c_{44} = 97.2 \text{ GPa}$$

<https://www.ctcms.nist.gov/~knc6/jsmol/JVASP-1001.html>



Classical potential (mod/c)

c_{11} (GPa)	172.6	165 ^a ; 167.40 ^b
c_{12} (GPa)	64.6	64 ^a ; 65.23 ^b
c_{44} (GPa)	81.3	79.2 ^a ; 79.57 ^b

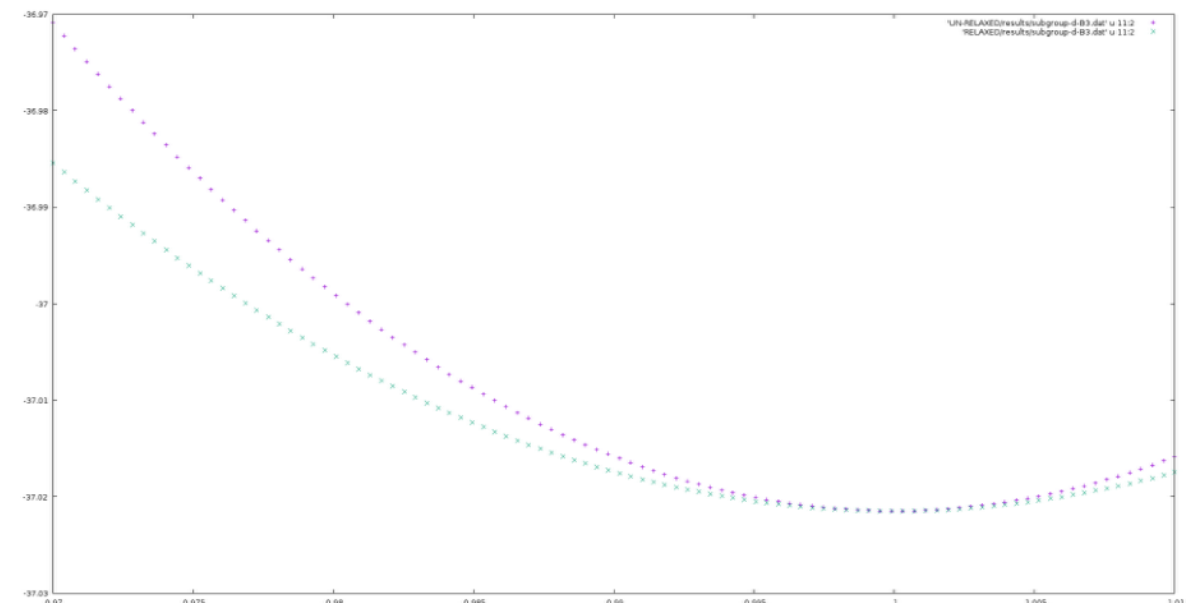
experiment

(no ionic relaxation)

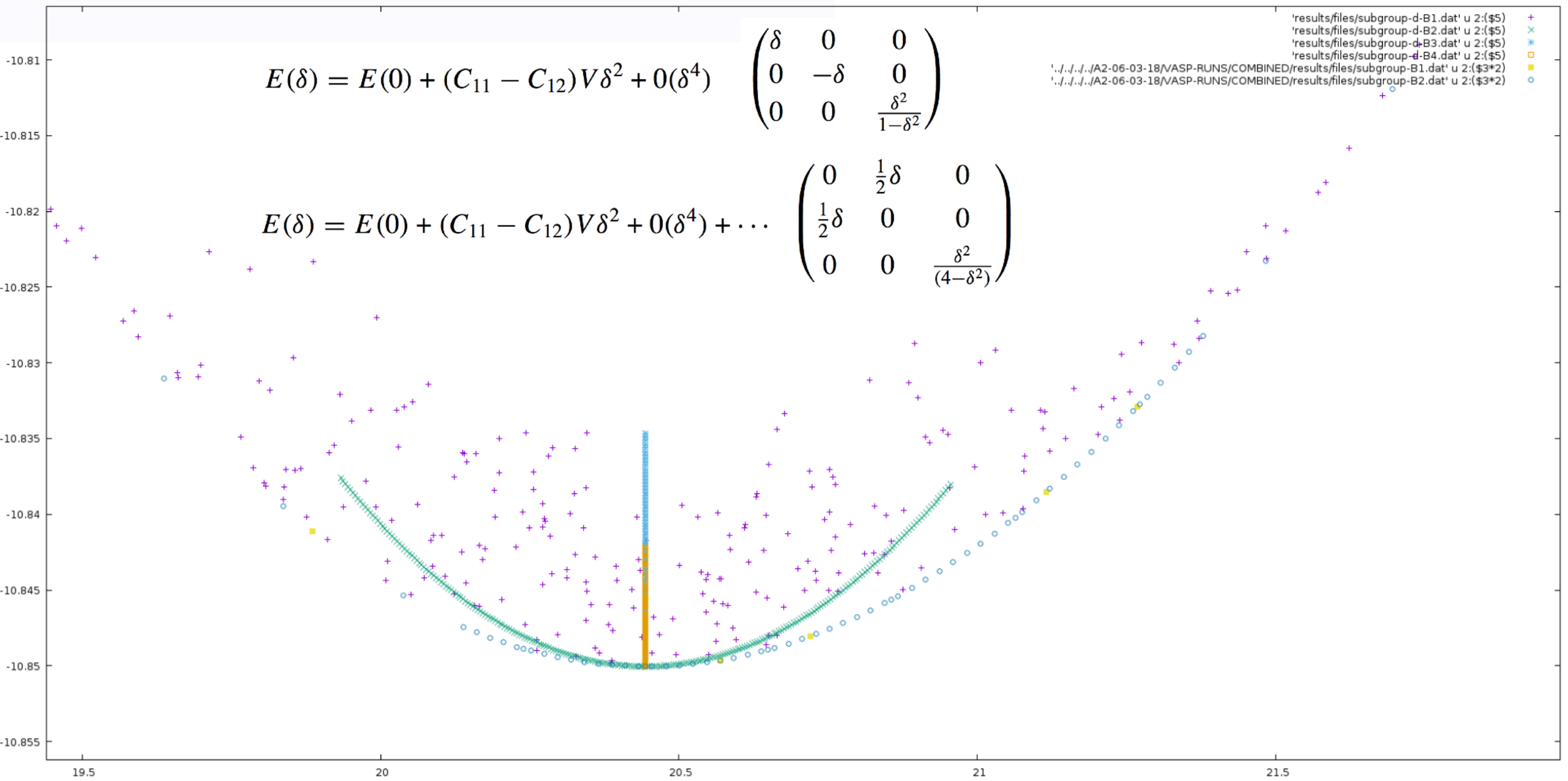
C11=171.554032204297 GPa
C12=66.5676160791408 GPa
C44=109.991181148439 GPa

(ionic relaxation)

C11=171.554032204157 GPa
C12=66.567616082438 GPa
C44=78.4100485501238 GPa

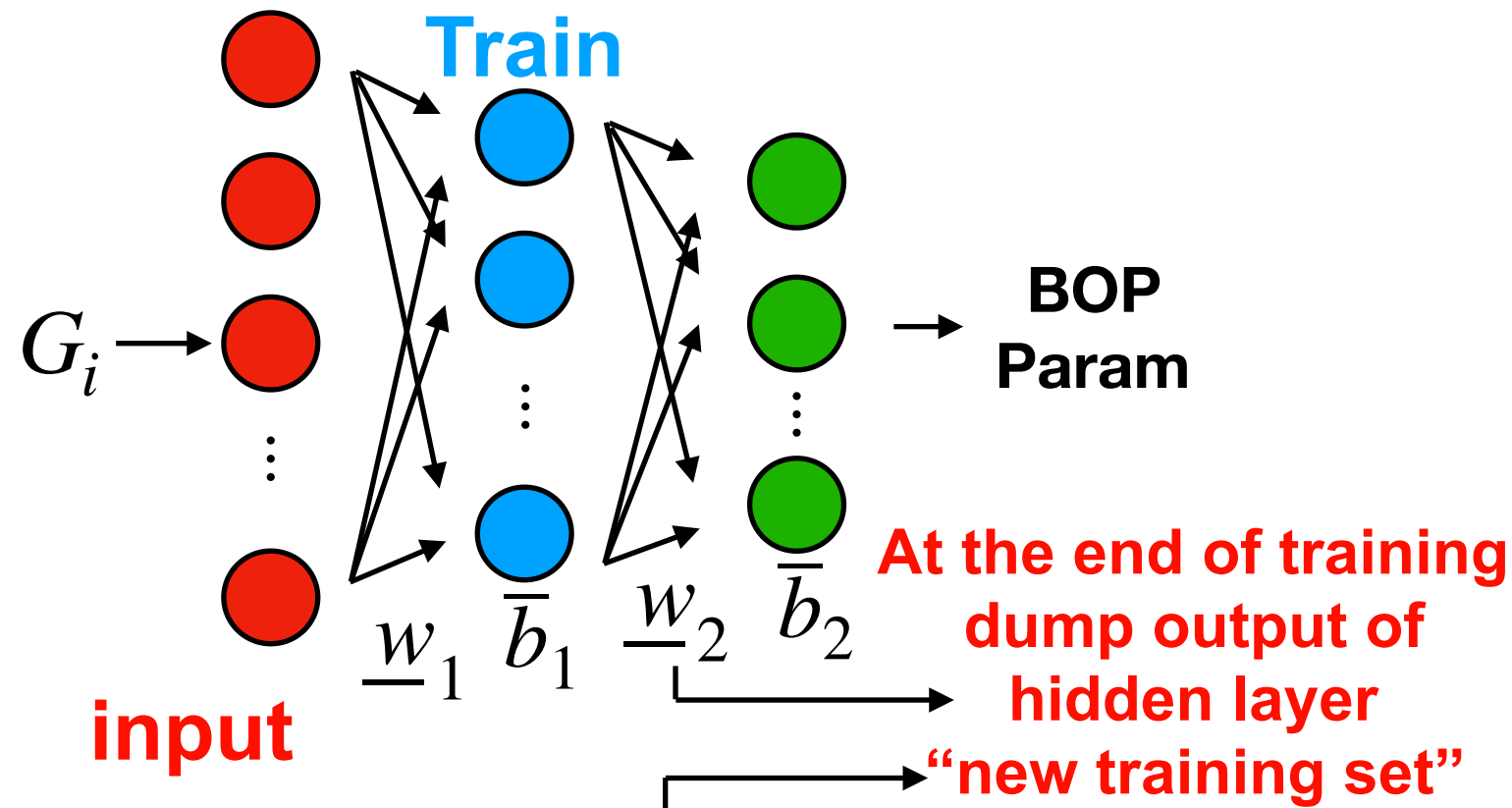


Elastic Constants

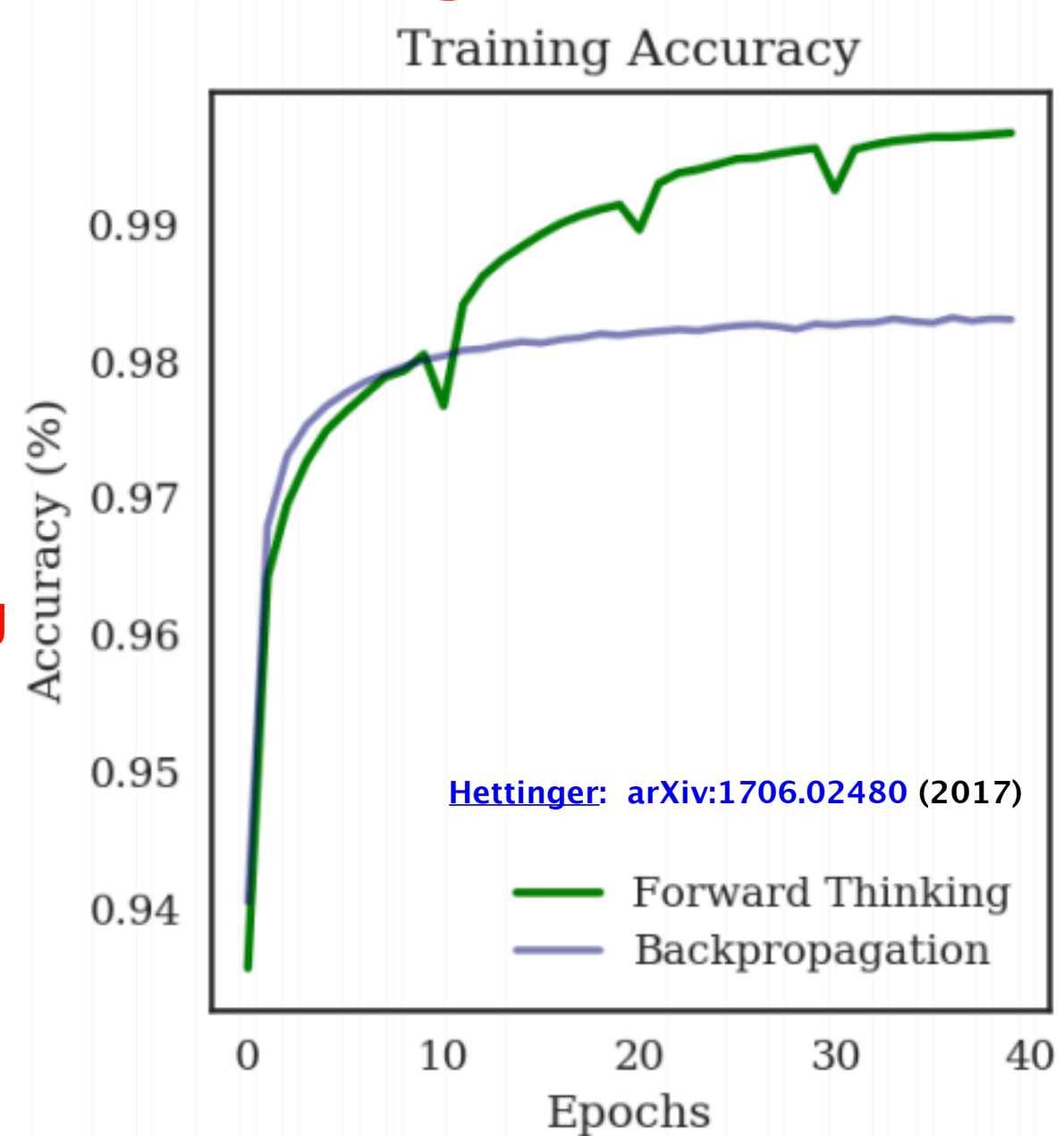
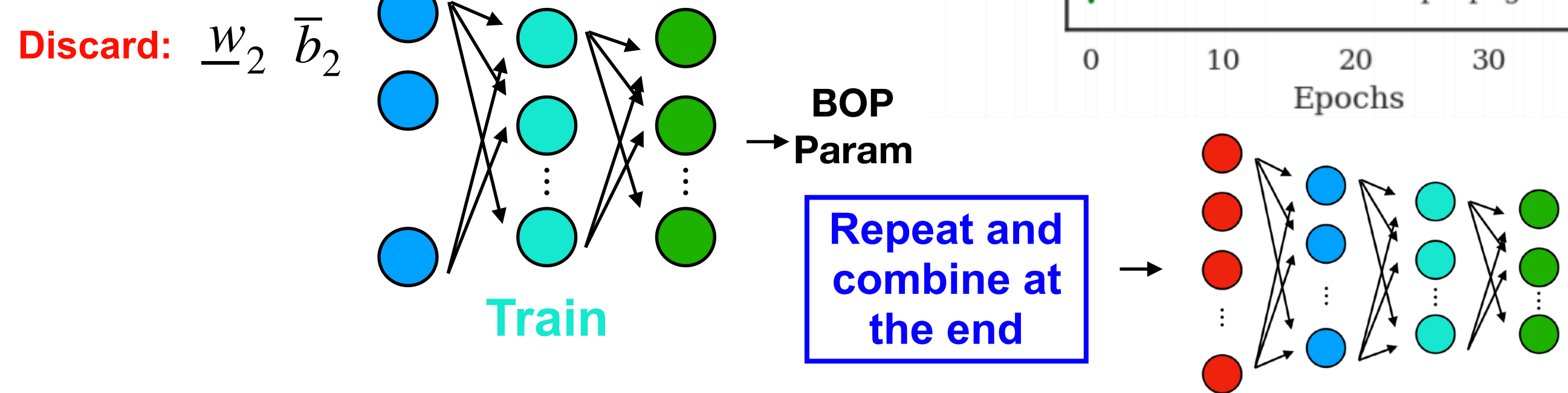


Future work-1: Forward thinking method

Stage-1



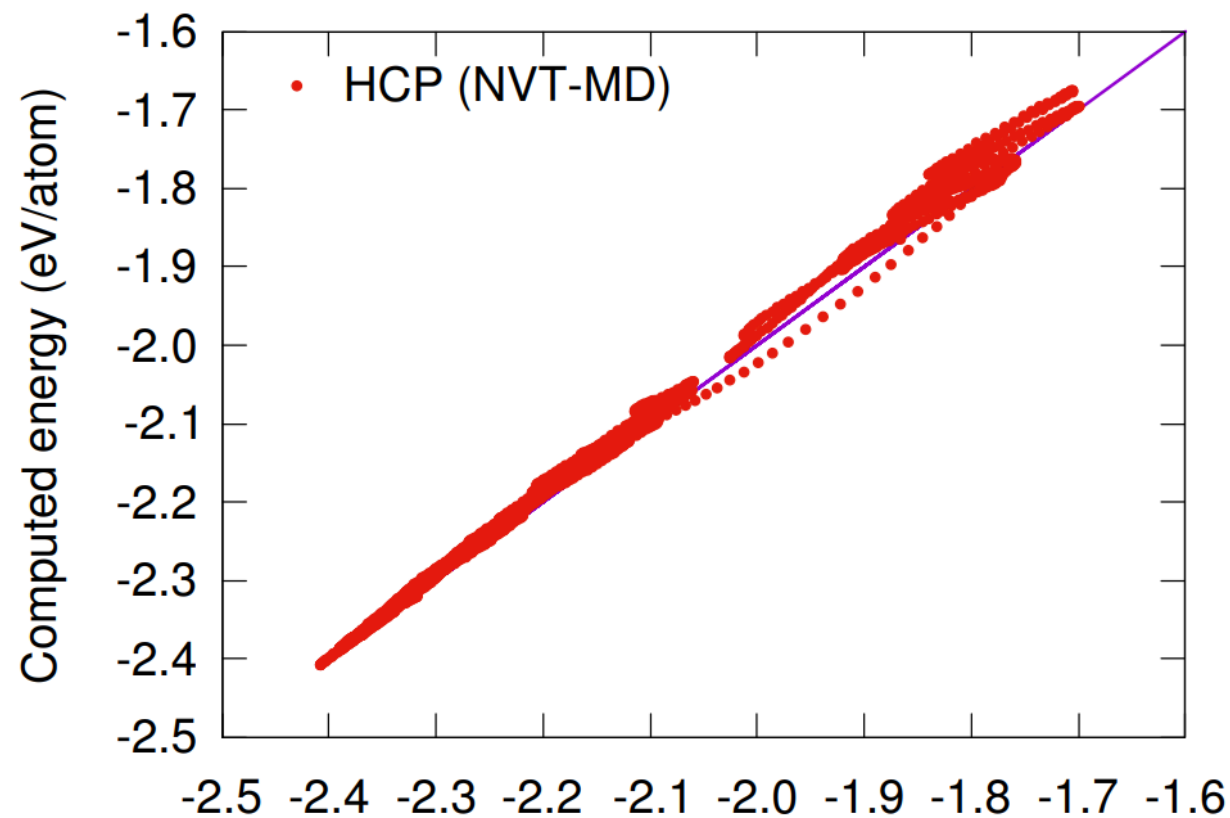
Stage-2



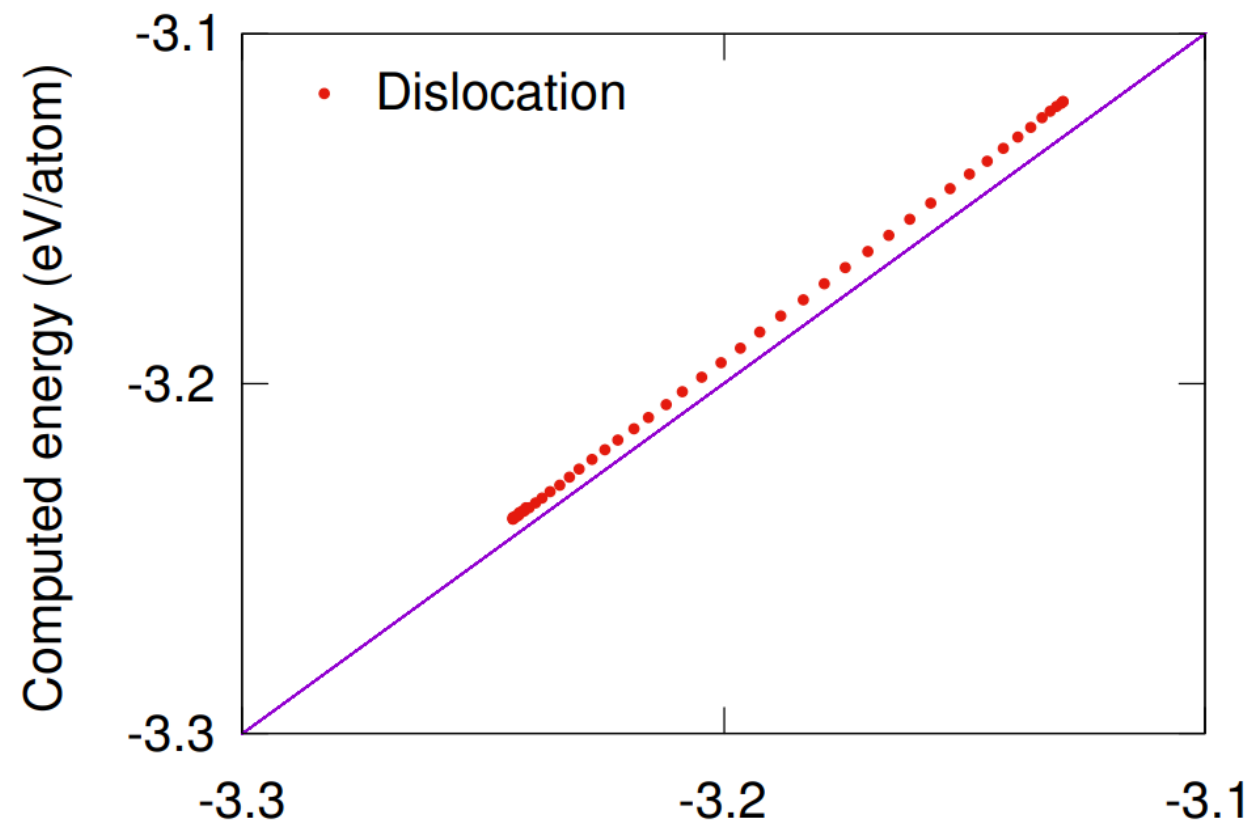
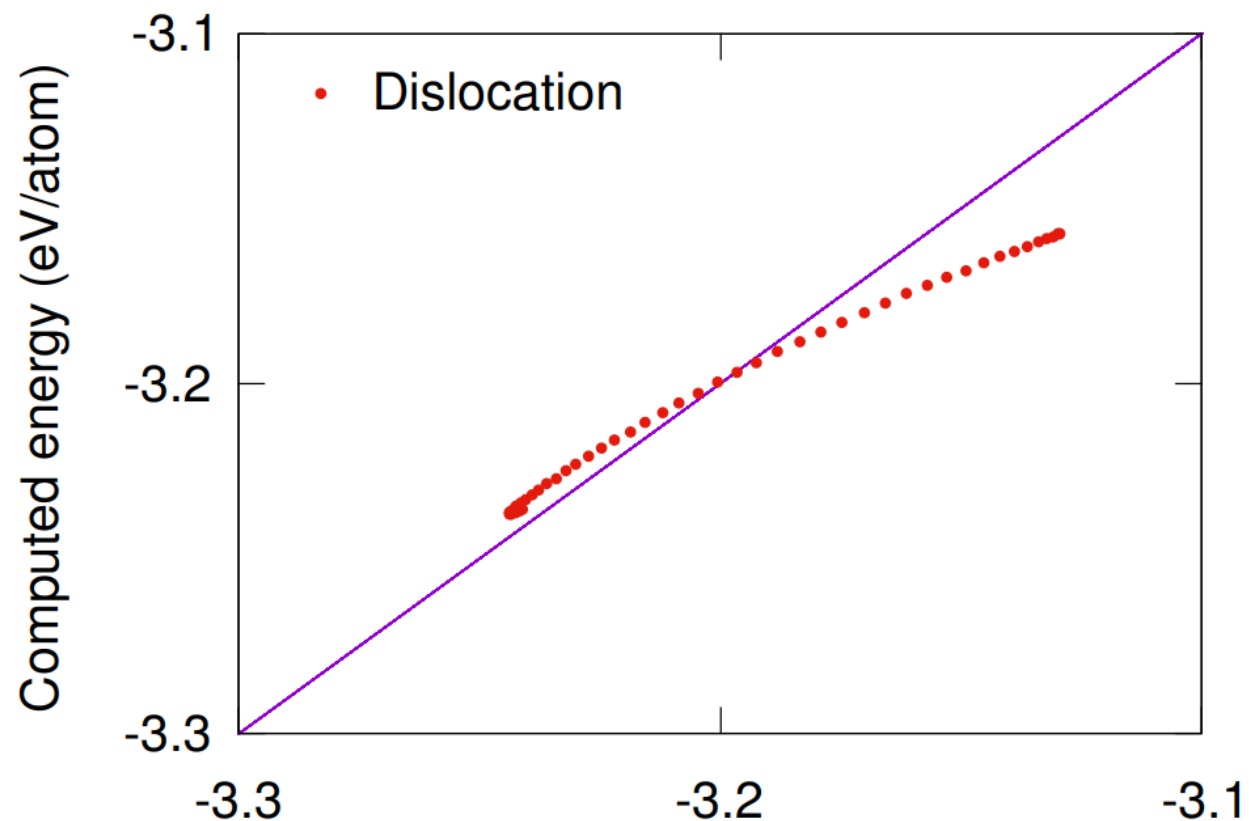
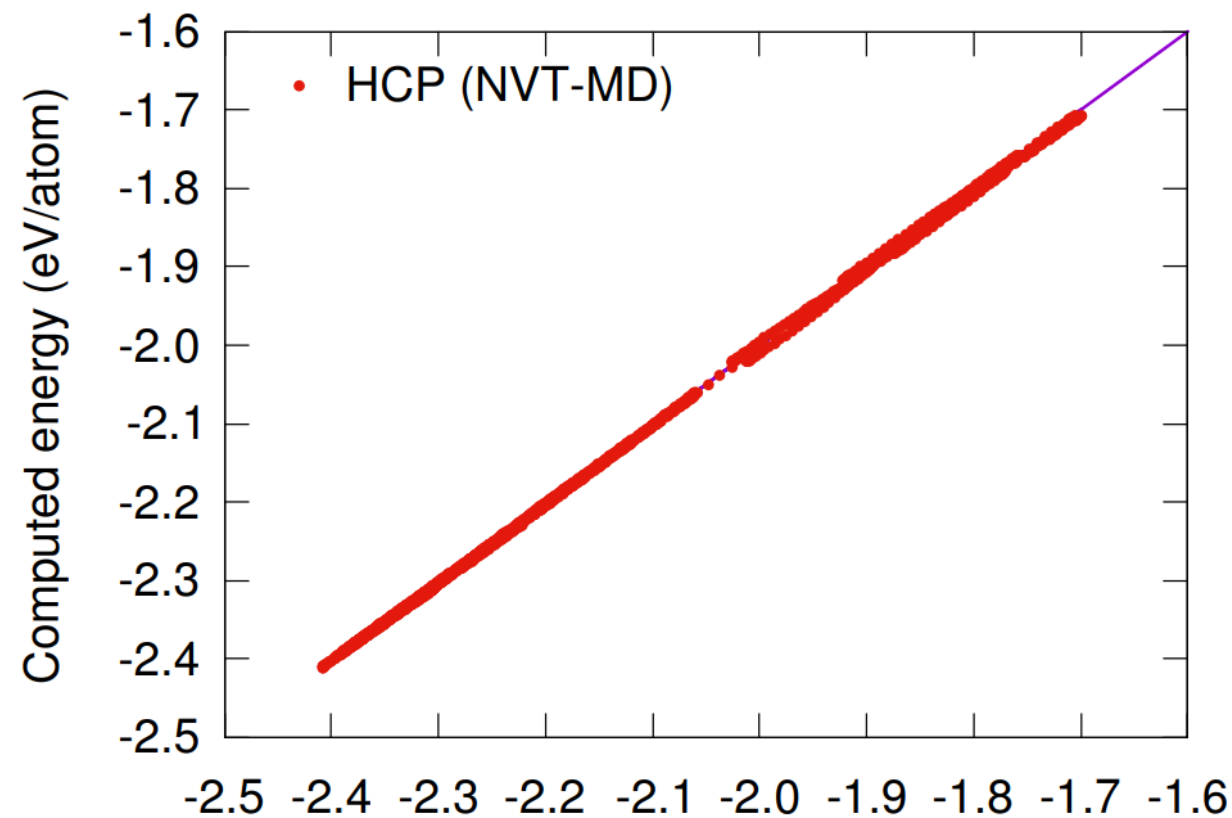
Dynamically build NN by training one layer at a time

Results: Aluminum NN and PINN Potential

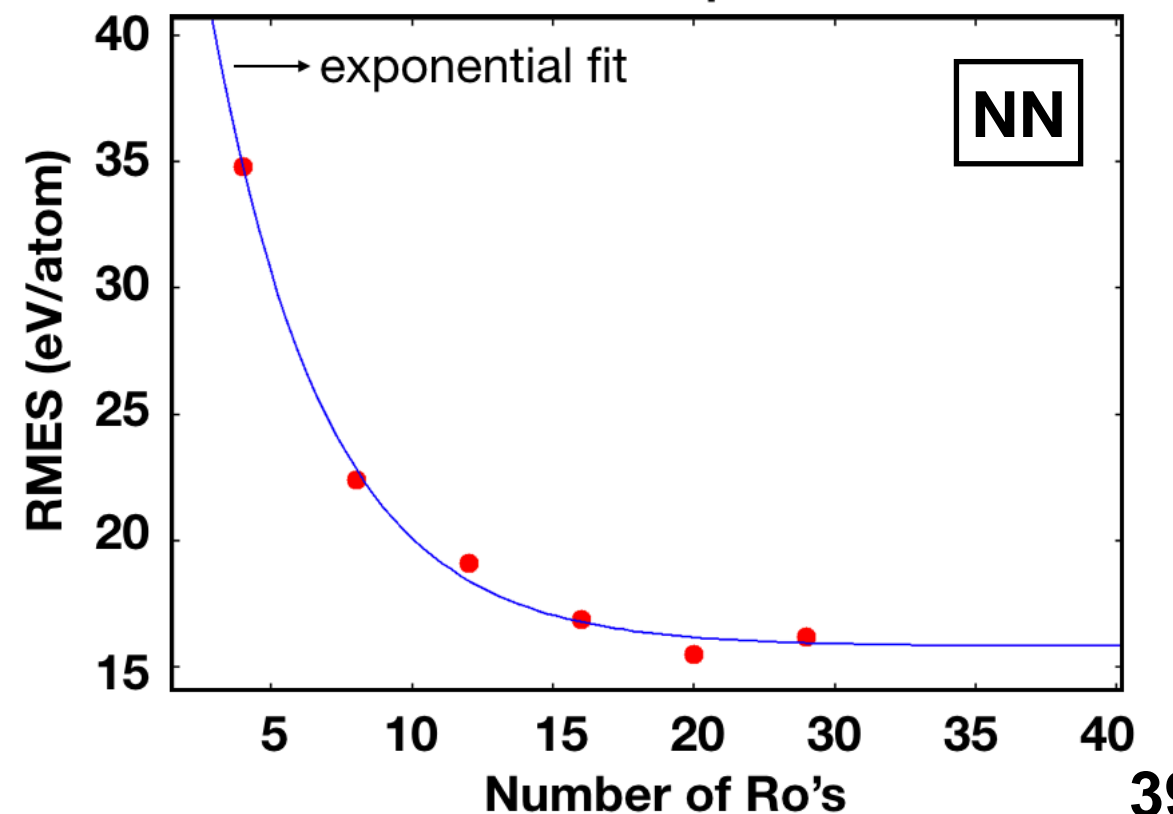
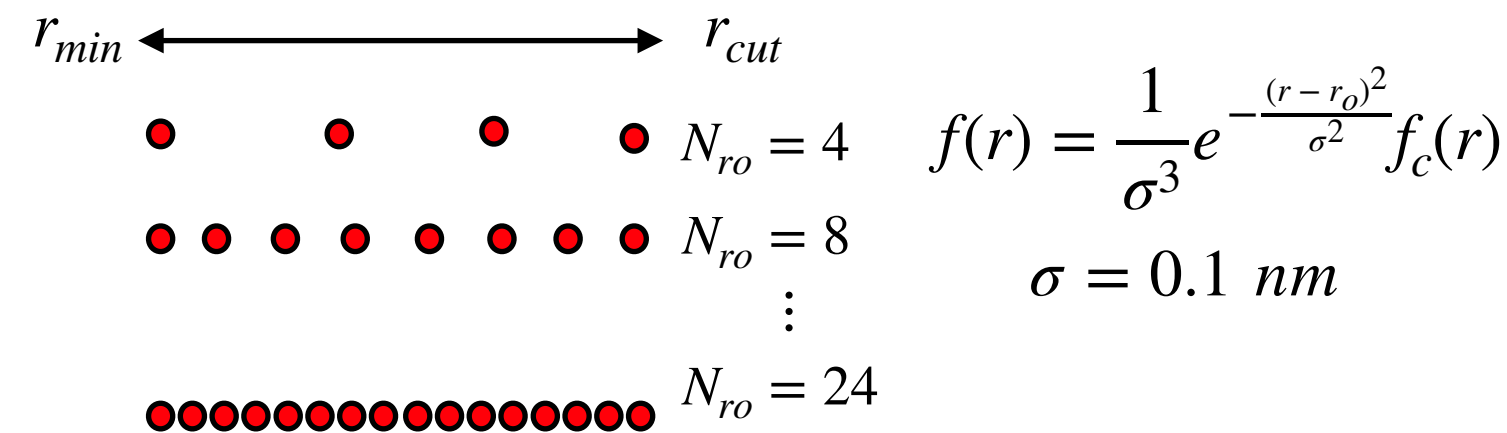
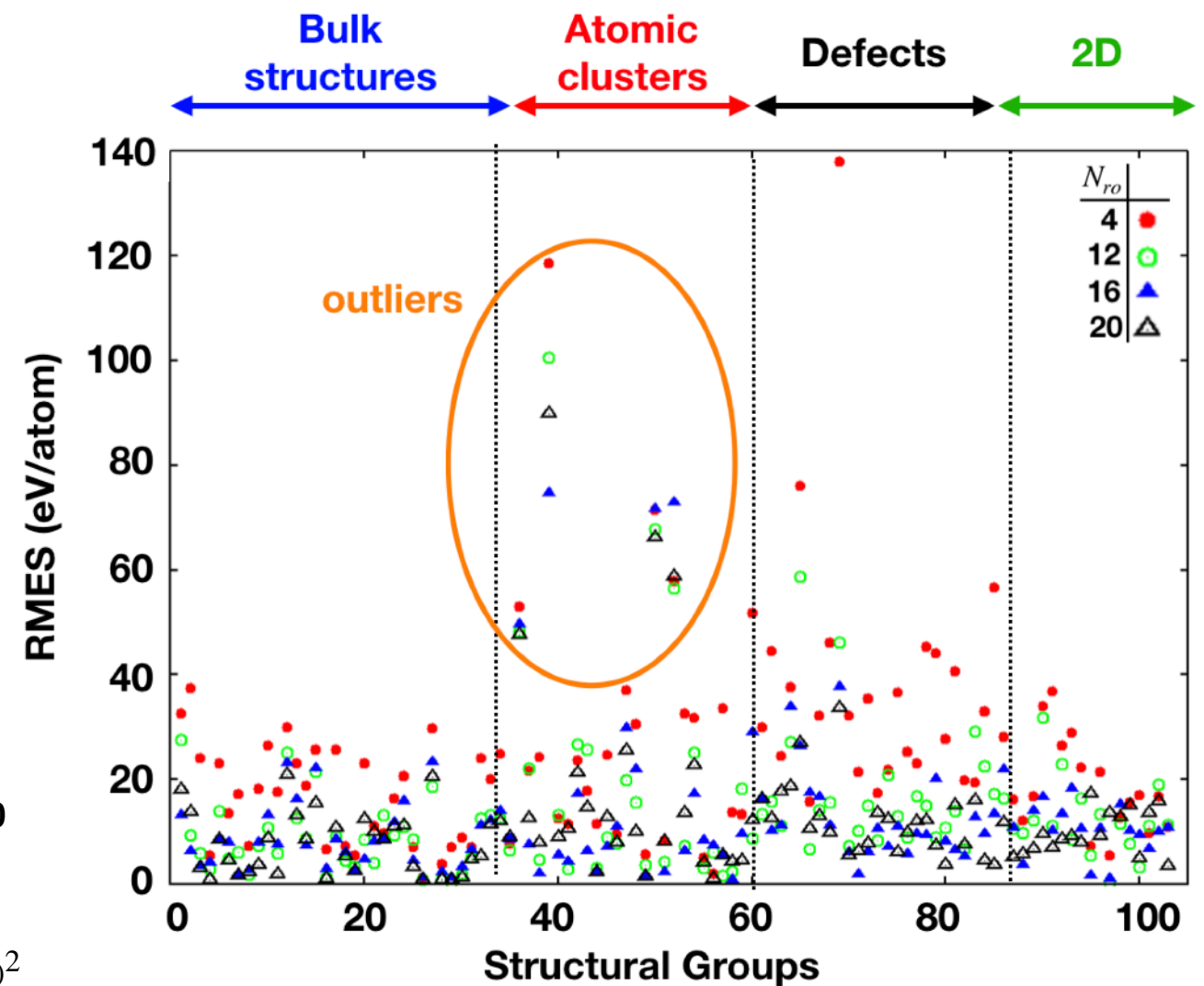
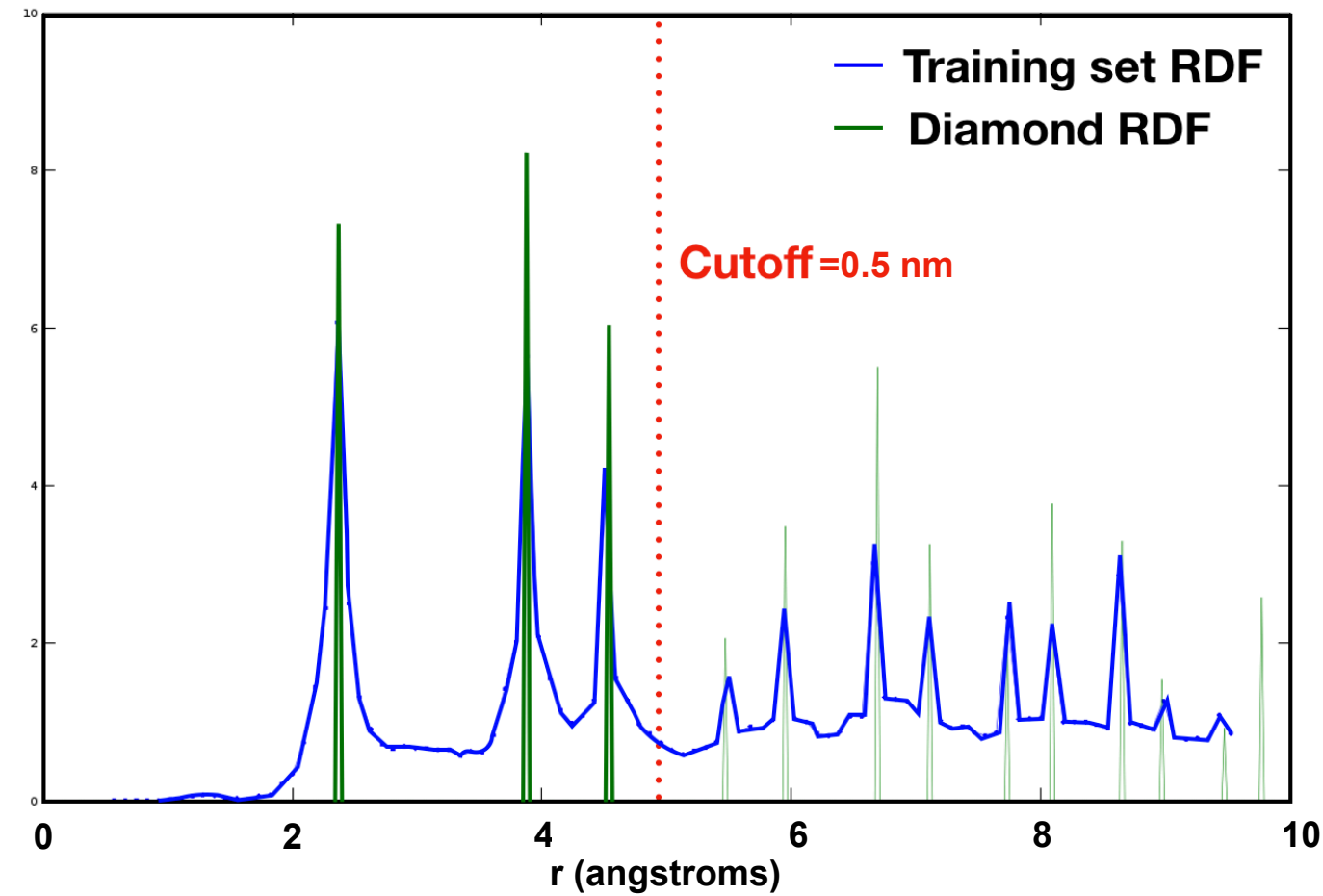
DFT energy (eV/atoms) (NN)



DFT energy (eV/atoms) (PINN)



Local structure parameter choice



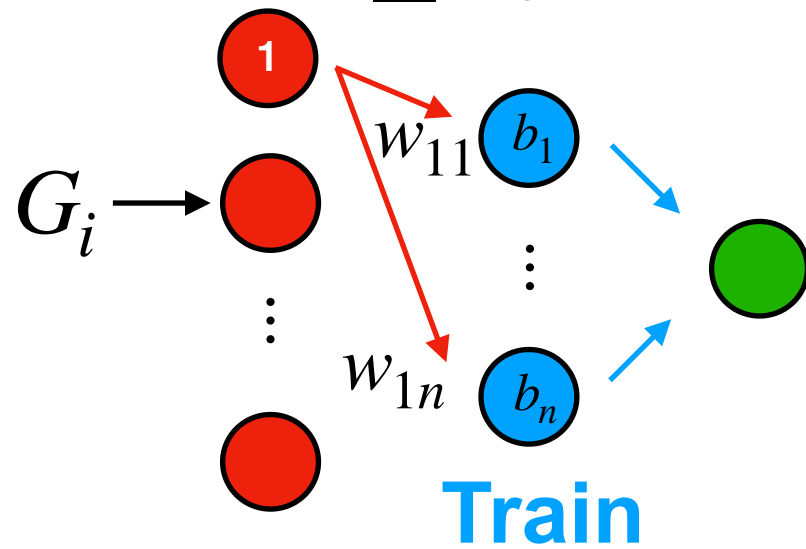
Observed a similar effect for PINN

Future work-1: Forward thinking method

Stage-1

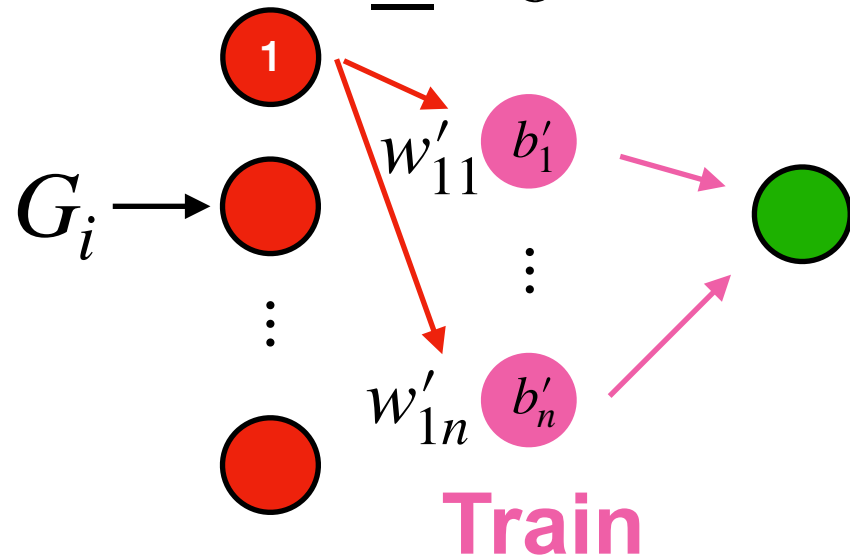
Diamond

$\underline{w} \quad \bar{b}$



FCC

$\underline{w}' \quad \bar{b}'$

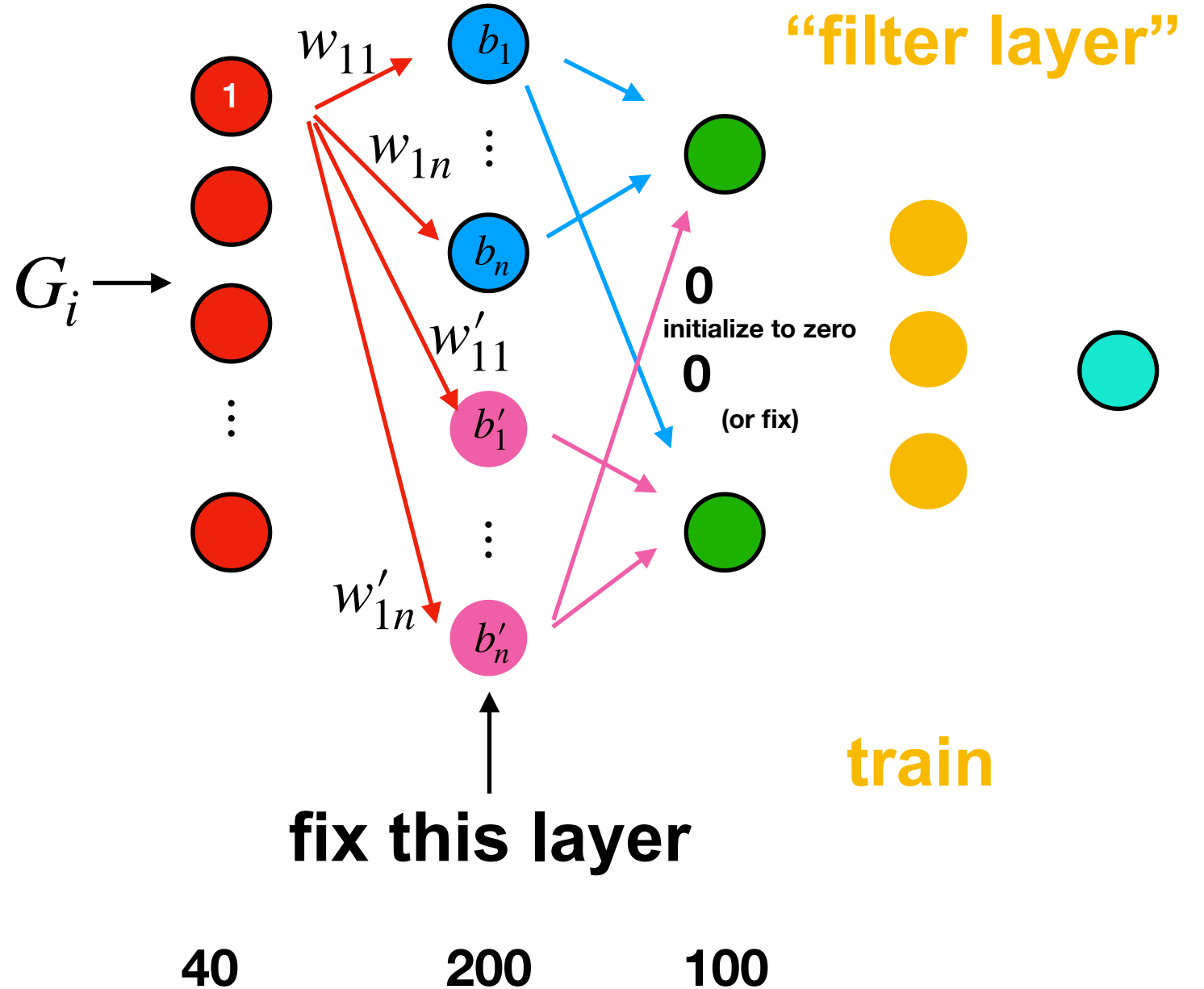


40-2-1

$(40 \cdot 2 + 2 + 2 + 1) = 85 \rightarrow (\sim 8500 \text{ fitting})$

Stage-2

$\underline{W} \quad \bar{B}$



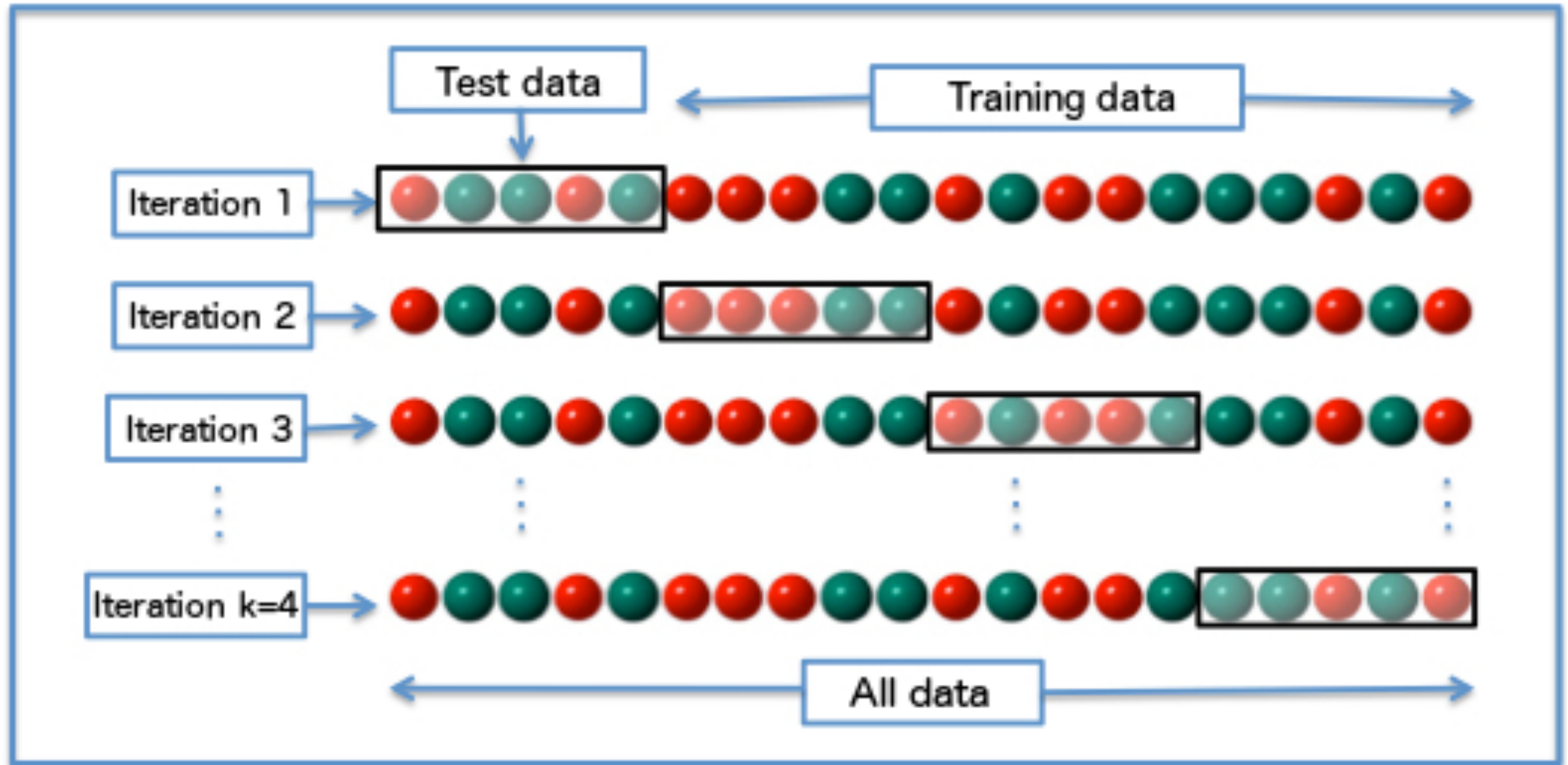
40

200

100

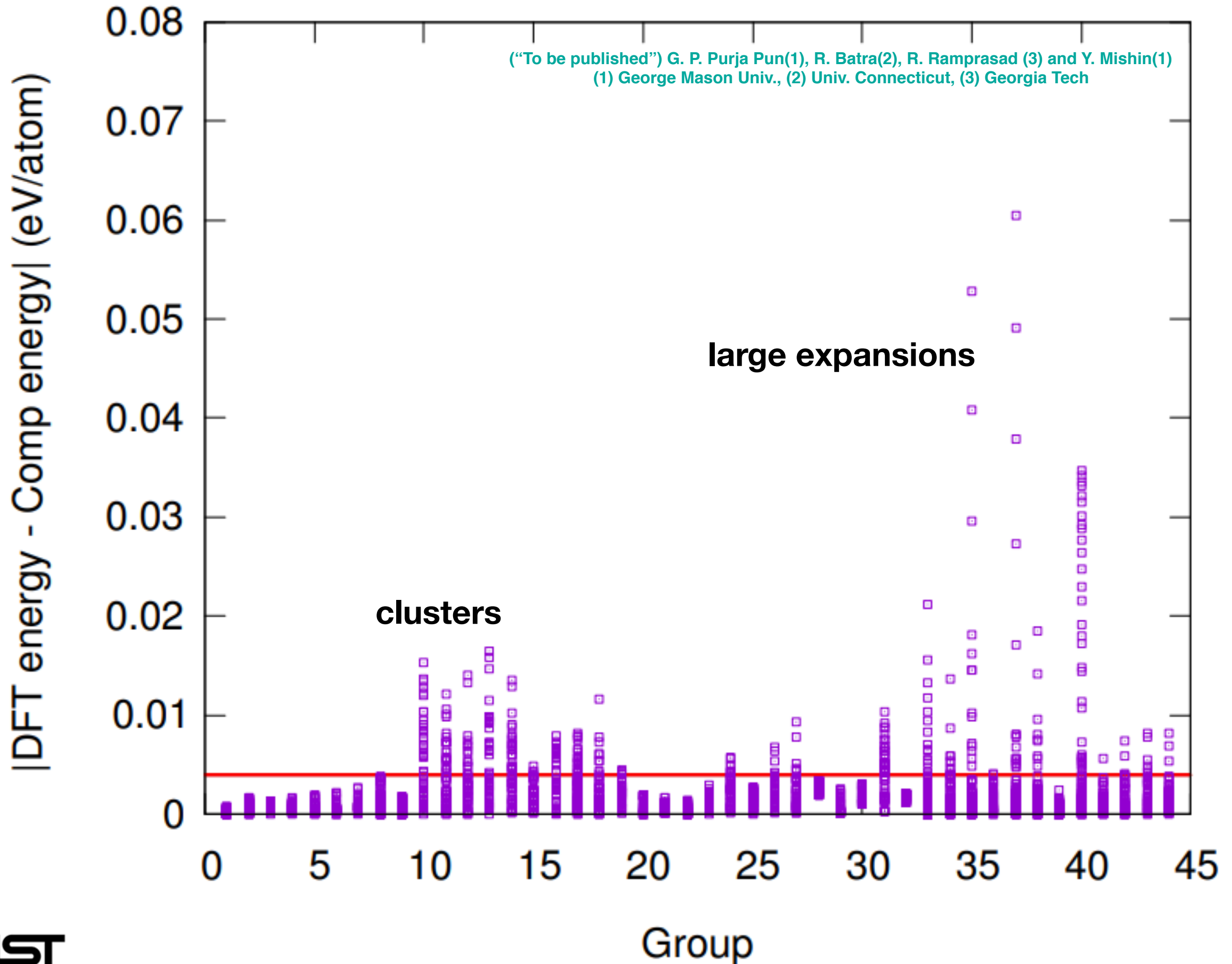
$(40 \cdot 2 + 2 + 2 + 1) = 85 \rightarrow (\sim 8500 \text{ fitting})$

K-fold validation

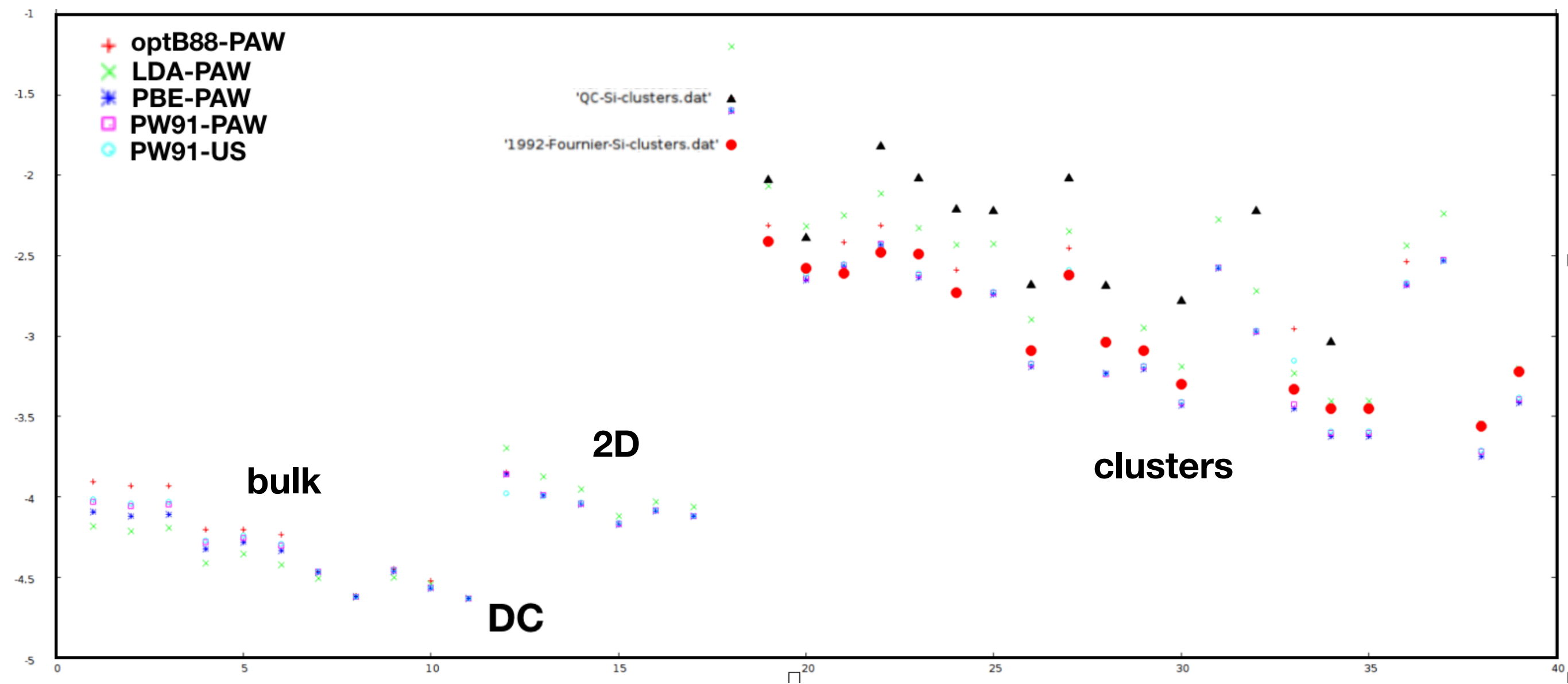


[https://en.wikipedia.org/wiki/Cross-validation_\(statistics\)](https://en.wikipedia.org/wiki/Cross-validation_(statistics))

Results: Aluminum PINN Potential



DFT variation



DFT variation

- **Points**
 - **Don't focus so much on details (wiggles, NN size)**
 - **Say humans and animals rather than just animals**
 - **pairwise repulsion, angular dependence, longer distance interactions, bond order effects, screening**